

Department of Electronic & Telecommunication
Engineering University of Moratuwa



BM4151 – Biosignal Processing

MATLAB Assignment 1
Digital filters

Palihakkara A.T. 170418E

This report is submitted in partial fulfillment of the requirements
for the module BM4151 Biosignal processing.

09 October 2021

List of Figures

Figure 1: Typical ECG Characteristics	4
Figure 2: Noisy ECG signal & the Ideal ECG signal.....	5
Figure 3: Power Spectral Density of ECG & noisy ECG signal	5
Figure 4: Comparing noisy ECG and delay compensated Filtered Signal.....	7
Figure 5: Compare Power Spectral Density Estimate of ma3ECG_1 and noisy ECG..	7
Figure 6: Comparing ECG_template, noisy ECG and ma3ECG_2.....	8
Figure 7: Magnitude Response, Phase Response & Pole - Zero Plot of MA(3) filter using fvtool.....	8
Figure 8: Magnitude Response, Phase Response & Pole - Zero Plot of MA(10) filter using fvtool.....	9
Figure 9: Comparing ECG_template, noisy_ECG, ma3ECG_2 and ma10ECG.....	9
Figure 10: Finding Optimum Moving Average filter	10
Figure 11: Applying Savitzsky Golay Filter (N,L)	11
Figure 12: Error vs Order of Savitzsky Golay Filters	11
Figure 13: Comparing ECG_template, sg310ECG and opt_sgECG.....	12
Figure 14: Comparing optimum MA and SG filter.....	12
Figure 15: ABR recording and Audio Pulse Stimuli	13
Figure 16: Zoomed Auditory Stimuli and EEG recording	13
Figure 17: Ensemble averaged ABR	14
Figure 18: MSE vs epochs.....	14
Figure 19: SNR variation vs epochs.....	15
Figure 20: ECG recording data set	16
Figure 21: ECG recording data set - scaled	16
Figure 22: Single ECG Waveform.....	17
Figure 23: Noisy ECG Dataset.....	17
Figure 24: Cross correlation with nECG & ECG template	17
Figure 25: Improvement of SNR.....	18
Figure 26: ECG Sample and Ensemble Average Comparison	18
Figure 27: xcorr pulse detection	19
Figure 28: Pole -Zero Plots of First Order Derivative and 3-point Central Difference Filters	21
Figure 29: Magnitude Response - Logarithmic Scale.....	21
Figure 30: Magnitude Response - Linear Scale	21
Figure 31: Unity Gain Magnitude Response - Linear Scale.....	22
Figure 32: Unity Gain Magnitude Response - Logarithmic Scale.....	23
Figure 33: Raw & Noisy ECG	23
Figure 34: Noisy ECG after applying the Filters	24
Figure 35: Filter Comparison (Zoomed)	24
Figure 36: Impulse Response of M=5,50,100 Filters	25
Figure 37: Magnitude Response of LP Filter using Rectangular Window M=5,50,100.....	25
Figure 38: Phase Response of LP Filter using Rectangular Window M=5,50,100 ..	26

Figure 39: Morphology of Rectangular, Hanning, Hamming and Blackman Filters	26
Figure 40: Logarithmic Magnitude Response of Rectangular, Hanning, Hamming and Blackman Filters.....	27
Figure 41:Linear Magnitude Response of Rectangular, Hanning, Hamming and Blackman Filters	27
Figure 42: Phase Response of Rectangular, Hanning, Hamming and Blackman Filters	27
Figure 43: Noisy ECG.....	28
Figure 44: PSD of Noisy ECG	28
Figure 45: Magnitude Response of LP and HP Filter	29
Figure 46: Phase Response of LP and HP Filter.....	30
Figure 47: Comb filter.....	30
Figure 48: LP Filtered ECG	30
Figure 49: LP & HP Filtered ECG.....	31
Figure 50: LP, HP and Comb Filtered ECG.....	31
Figure 51: Casacade Filter Magnitude and Phase Response	31
Figure 52: PSD comparison of Filtered Signal and Noisy signal.....	32
Figure 53: Magnitude and Phase Response of Butterworth LP Filter M =453	33
Figure 54: Group Delay Response of Butterworth LP Filter M =453	33
Figure 55: IIR BW LP Filter Magnitude & Phase Response M = 10	34
Figure 56: IIR BW LP Filter Group Delay M = 10	34
Figure 57: IIR BW HP Filter Magnitude & Phase Response M = 10	34
Figure 58: IIR BW HP Filter Group Delay M = 10	35
Figure 59: IIR BW Comb Filter Magnitude & Phase Response M = 10	35
Figure 60: IIR BW Comb Filter Group Delay M = 10.....	35
Figure 61: Magnitude Response Comparison.....	36
Figure 62: Forward Filtered Signal.....	36
Figure 63: Forward Filtered (Zoomed).....	37
Figure 64: Forward-Backward Filtered Signal.....	37
Figure 65: Forward-Backward Filtered Signal (Zoomed)	38
Figure 66: Filter Comparison	38
Figure 67: PSD Comparison.....	39

1. Smoothing Filters

1.1. Moving Average Filter

$$y(n) = \frac{1}{N} \sum_{k=0}^{N-1} x(n-k)$$

Moving Average Filter is designed and implemented according to the above equation. Here we are using a “ECG_template.mat” and then add 5 dB Gaussian Noise to that data set to obtain a noisy ECG signal. After that we apply the designed Moving Average Filter and observe the characteristics of the signal.

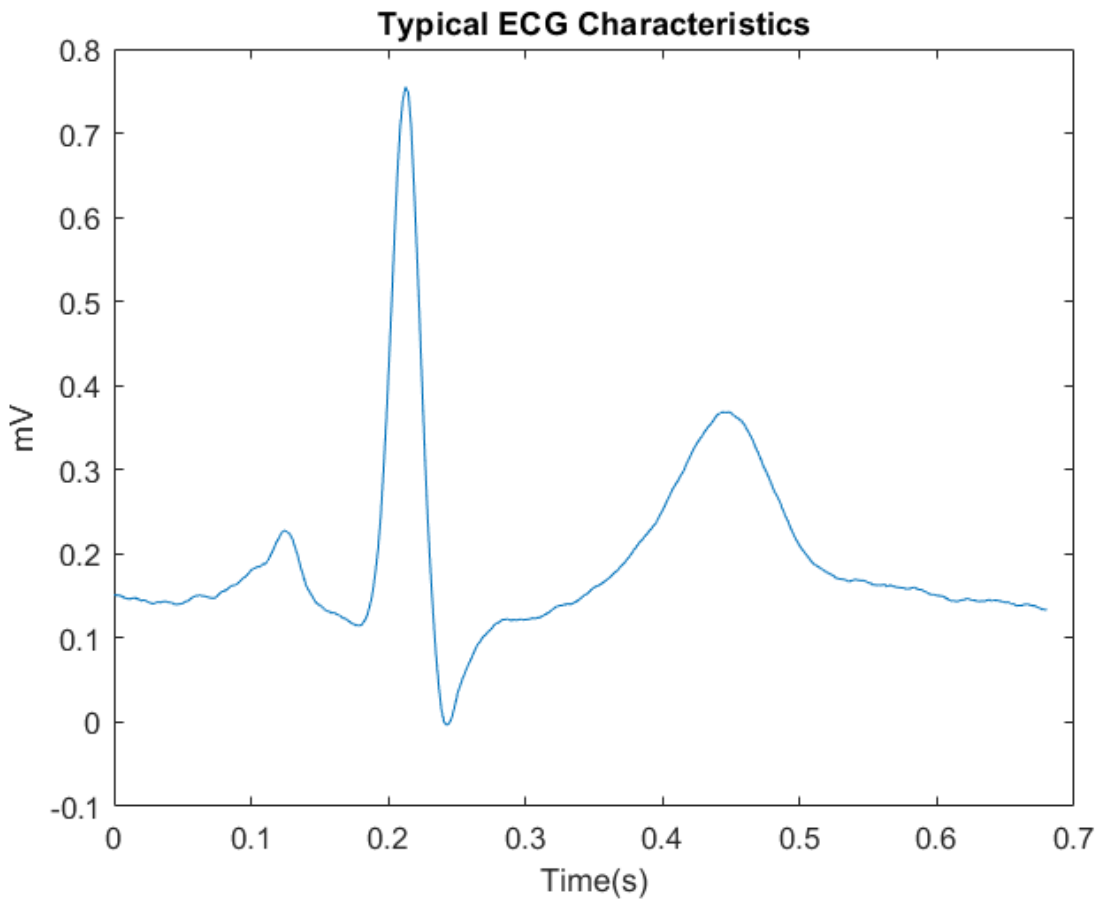


Figure 1: Typical ECG Characteristics

After adjusting the time scale with the sampling frequency of 500 Hz, we can observe an ECG pulse as shown in Figure 1. In there we can clearly observe the P wave, QRS complex and the T wave of a typical ECG signal.

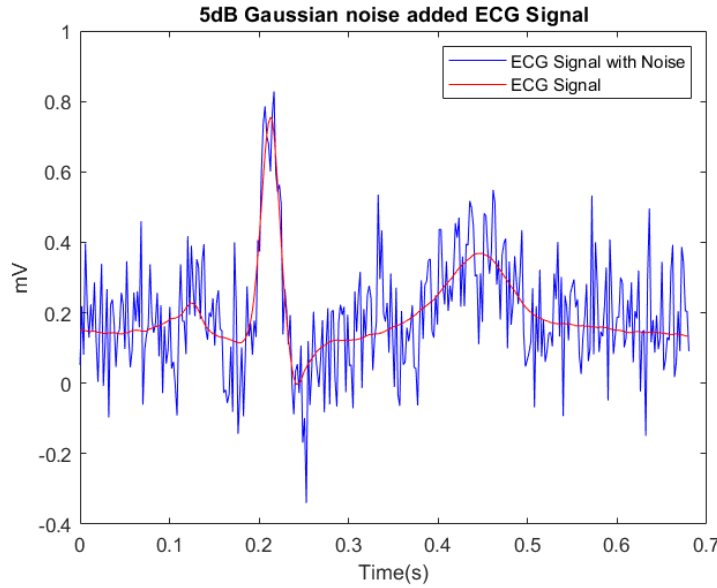


Figure 2: Noisy ECG signal & the Ideal ECG signal

5 dB Gaussian Noise is added to the ECG_template data set using “awgn(x, snr, ‘measured’)” function and both noisy signal and the reference signal is plotted in a single figure as in Figure 2.

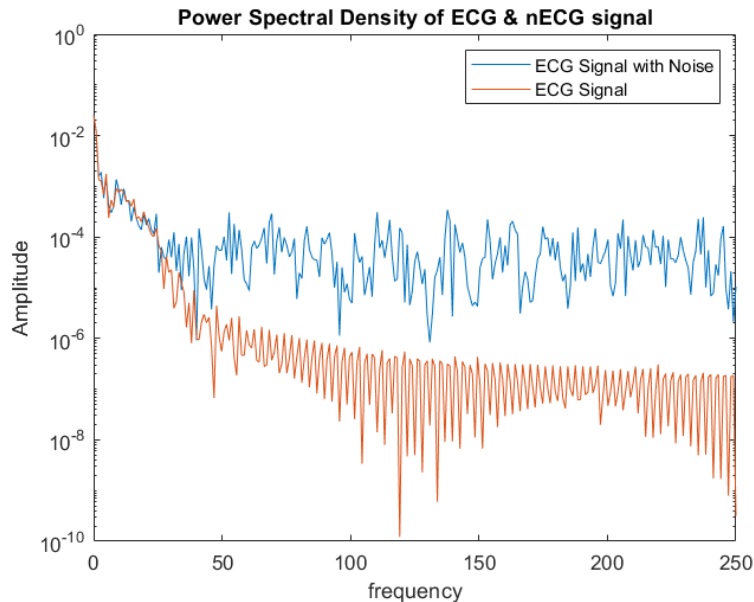


Figure 3: Power Spectral Density of ECG & noisy ECG signal

Power Spectral Density gives the signal power in different frequency components of a signal. When looking into the Figure 3, we can clearly see that, the ECG signal power is prominent in the lower frequencies (< 50 Hz) and the noisy ECG signal has more power in high frequencies due to the added noise.

Moving Average Filter Implementation

Derive the Group Delay

Let's derive the transfer function of the filter.

$$y(n) = \frac{1}{N} \sum_{k=0}^{N-1} x(n-k) \xrightarrow{\mathcal{F}} Y(\omega) = \frac{1}{N} \sum_{k=0}^{N-1} X(\omega) z^{-k}$$

$$H(\omega) = \frac{Y(\omega)}{X(\omega)} = \frac{1}{N} \sum_{k=0}^{N-1} z^{-k}$$

$$H(\omega) = \frac{1}{N} \sum_{k=0}^{N-1} e^{-j\omega k}$$

$$H(\omega) = \frac{e^{-j(\frac{N-1}{2})\omega}}{N} \sum_{k=-(N-1)/2}^{(N-1)/2} e^{-j\omega k}$$

Since, $e^{j\theta} = \cos \theta + j \sin \theta$, the above equation can be simplified as,

$$H(\omega) = \frac{\cos\left(\frac{N-1}{2}\right)\omega - j \sin\left(\frac{N-1}{2}\right)\omega}{N} \sum_{k=-(N-1)/2}^{(N-1)/2} 2 \cos k\omega$$

$$\text{Arg}(H(\omega)) = \tan^{-1}\left(\frac{\text{Im}(H(\omega))}{\text{Re}(H(\omega))}\right)$$

$$\text{Arg}(H(\omega)) = \tan^{-1}\left(\frac{\cos\left(\frac{N-1}{2}\right)\omega}{-\sin\left(\frac{N-1}{2}\right)\omega}\right)$$

$$\text{Arg}(H(\omega)) = \tan^{-1}\left(\tan\left(\pi + \left(\frac{N-1}{2}\right)\omega\right)\right)$$

$$\text{Arg}(H(\omega)) = \pi + \left(\frac{N-1}{2}\right)\omega$$

The group delay is defined as,

$$\text{Group Delay } (\tau_g) = \frac{\partial \text{Arg}(H(\omega))}{\partial \omega}$$

$$\therefore \text{Group Delay } (\tau_g) = \frac{N-1}{2}$$

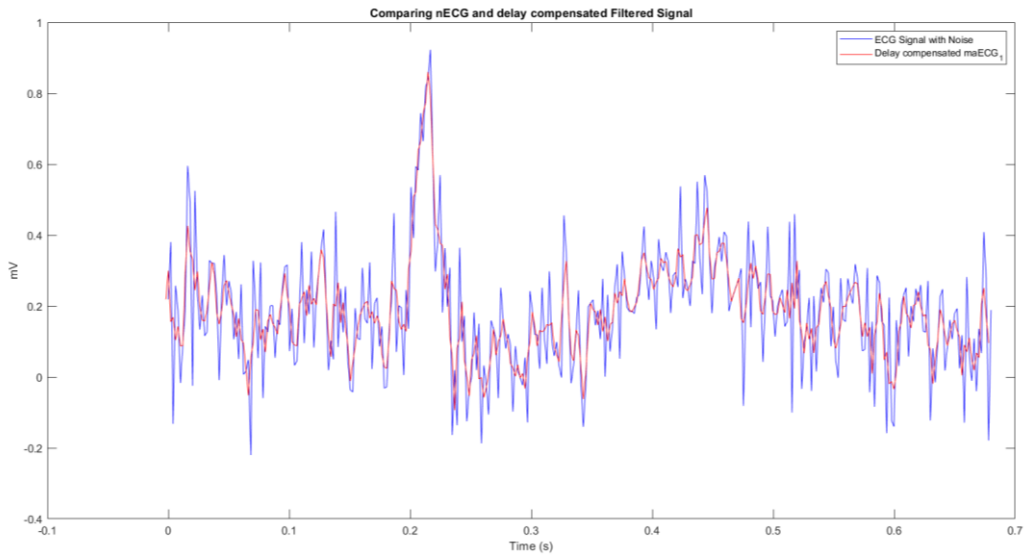


Figure 4: Comparing noisy ECG and delay compensated Filtered Signal

After compensating the group delay, we can see that both signals get aligned in the time domain and after applying the Moving Average filter, signal has smoothened by reducing the high frequency variation.

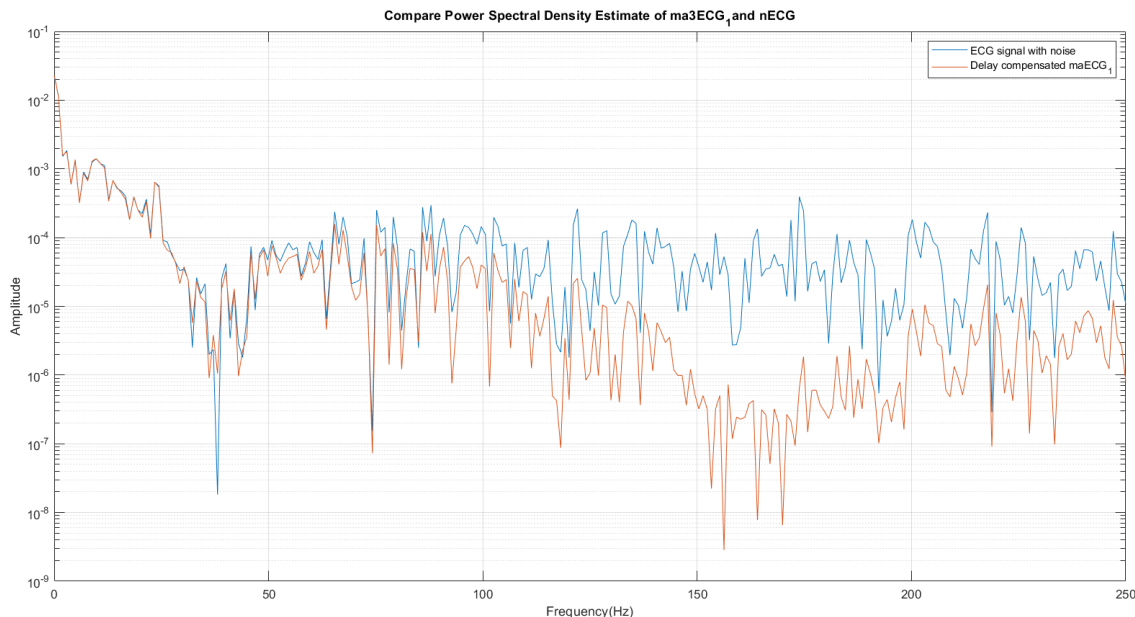


Figure 5: Compare Power Spectral Density Estimate of ma3ECG_1 and noisy ECG

Figure 5 drastically shows that the removal of high frequency components of the signal after applying the Moving Average filter. The signal power in high frequencies is reduced but the low frequencies (<50 Hz) are not affected by the filter.

Moving Average Filter Implementation using built-in function

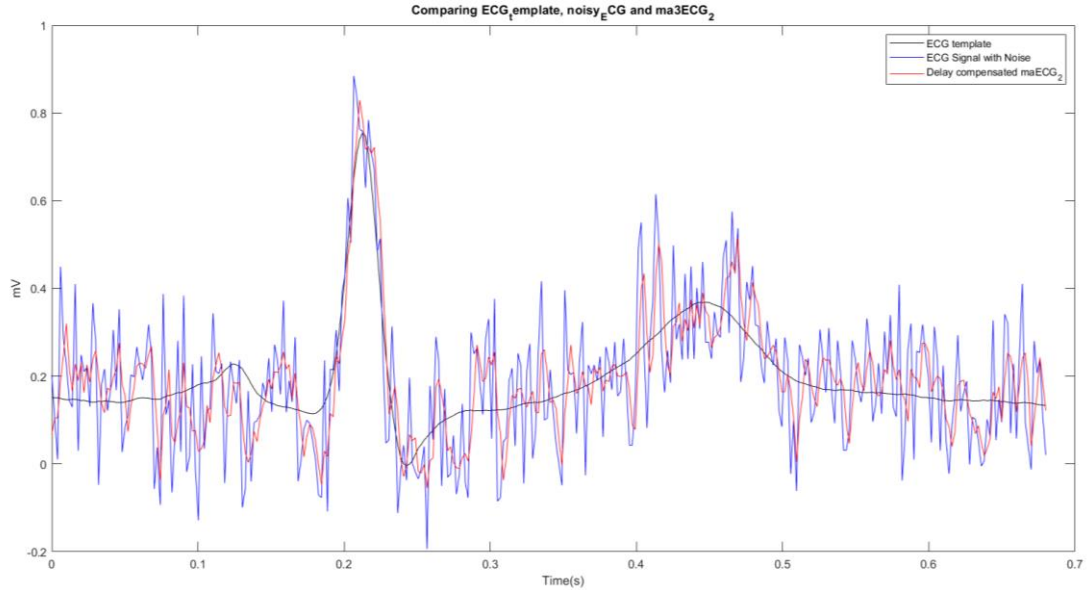


Figure 6: Comparing ECG_template, noisy ECG and ma3ECG_2

The filtered signal has smoothed the noisy signal by reducing high frequency variations like in the signal filtered using the derived Moving Average Filter (Figure 4).

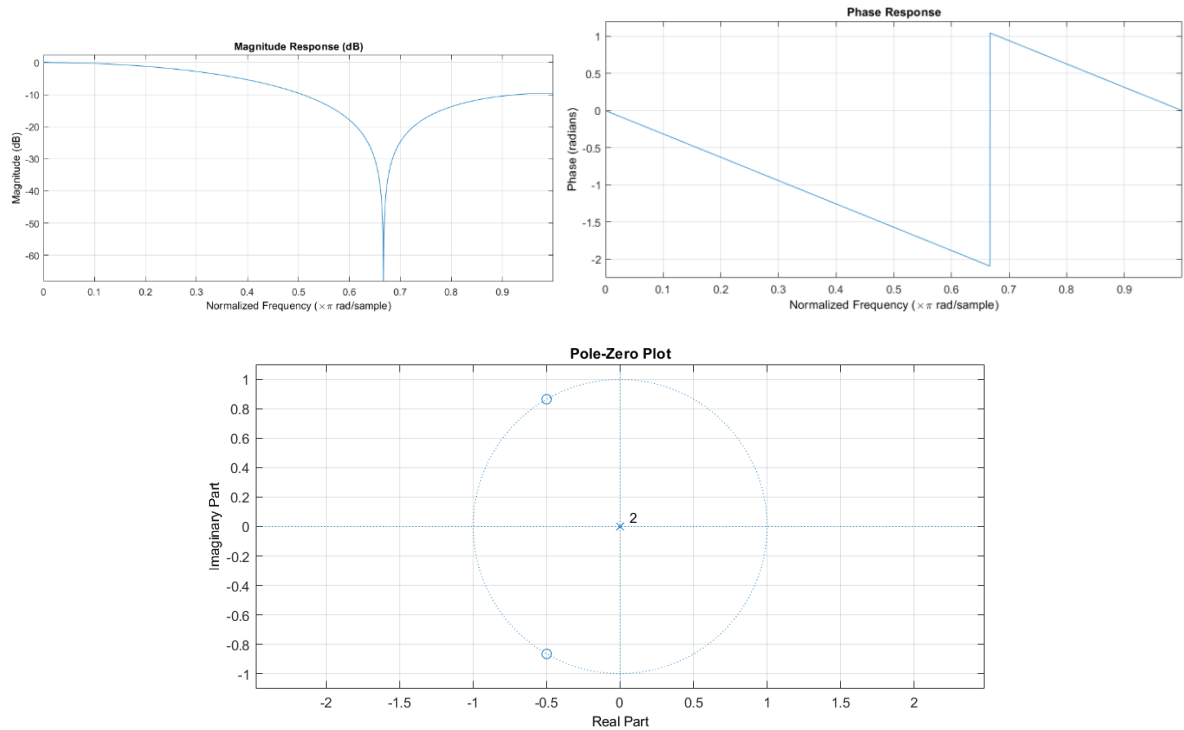


Figure 7: Magnitude Response, Phase Response & Pole - Zero Plot of MA(3) filter using fvtool

MA(10) filter implementation with the built-in function

By increasing the order of the filter, we are using higher number of points to obtain the average. And that will reduce more amount of high frequency noise in the signal.

The response of the MA(3) crosses the threshold of -3dB magnitude around 0.3 of the normalized frequency, while for MA(10), frequencies above 0.03 of the normalized frequency is cut-off.

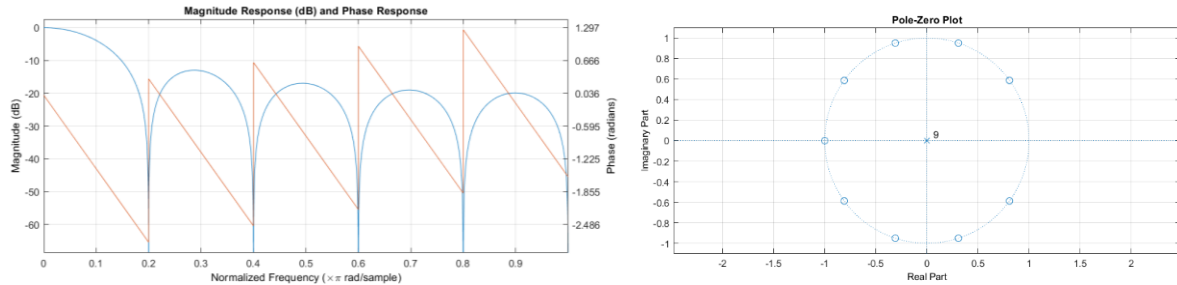


Figure 8: Magnitude Response, Phase Response & Pole - Zero Plot of MA(10) filter using fvtool

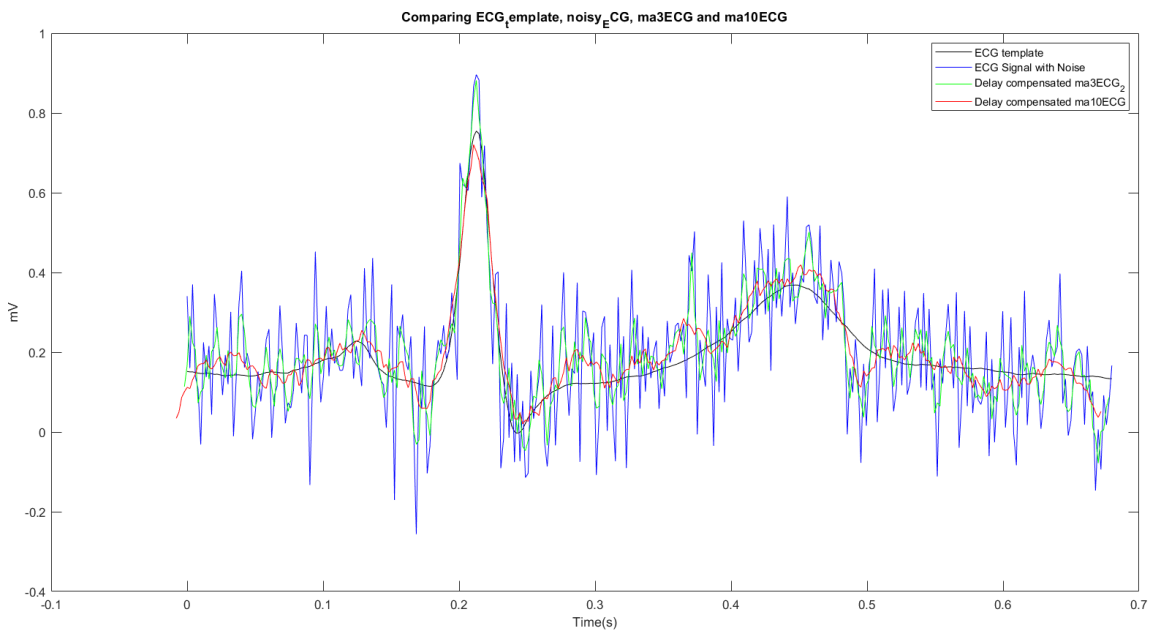


Figure 9: Comparing ECG_template, noisy_ECG, ma3ECG_2 and ma10ECG

As supposed, the ECG signal filtered by MA(10) filter is more smoother than the MA(3) filtered signal and the noisy ECG signal. Also, it has low number of high frequency noise compared to the other noisy signals. Due to the averaging the MA(10) filter itself smooth the peaks of the signal, additionally.

Optimum MA(N) filter order

Lower order Moving Average filtered signals may contain considerable amount of high frequency noise while high order moving average filters may remove the original signal components apart from the noise components. So, finding an optimum order for a moving average filter will lead to a best filtered signal.

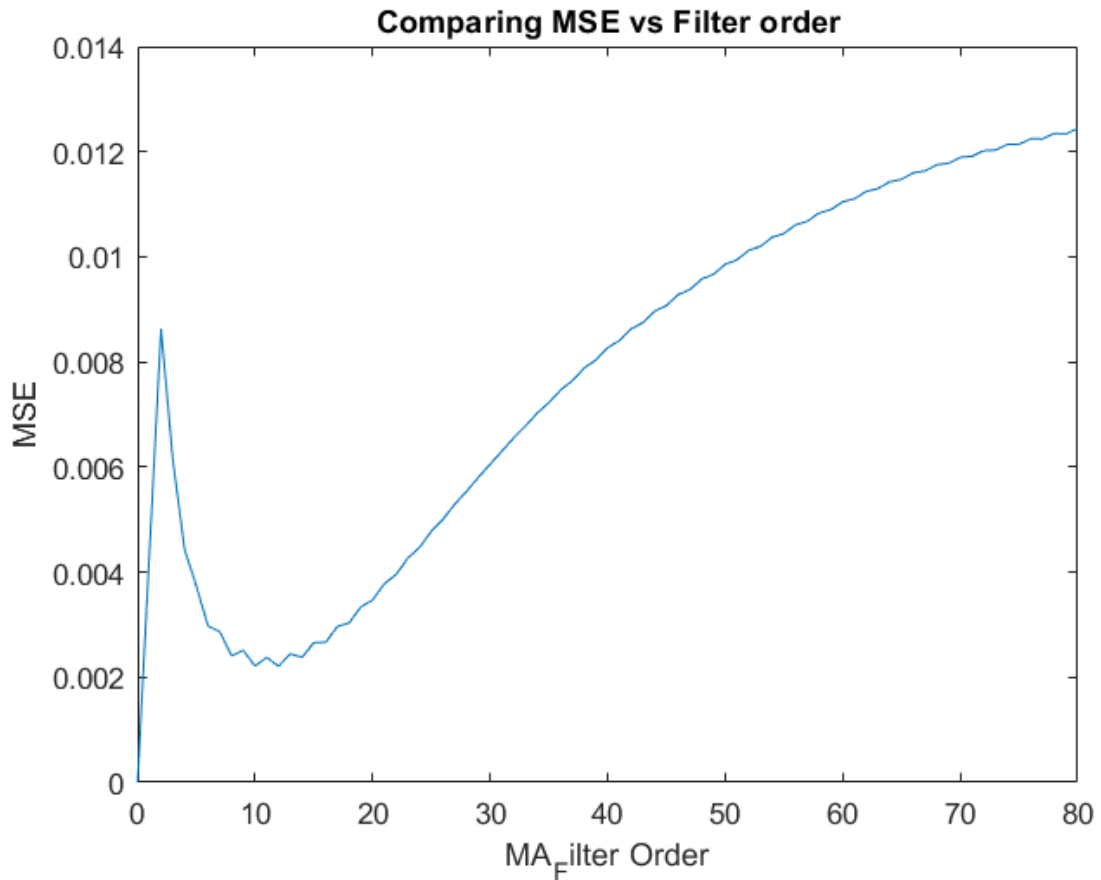


Figure 10: Finding Optimum Moving Average filter

Observed Optimum Filter Order = 12

With high filter orders, the window will use higher number of data points to calculate the average of a point. And it may lead to giving a more global average while compensating the signal data points over noise components. Due to that reason higher filter orders show high Mean Squared Error values.

1.2. Savitzky-Golay SG(N, L) filter

Savitzky-Golay filter fits a polynomial of order N to an odd number of data points $L' = 2L+1$ (where L' is an odd integer) in predefined window in a least-squares sense. A unique solution requires $N \leq L' - 1$.

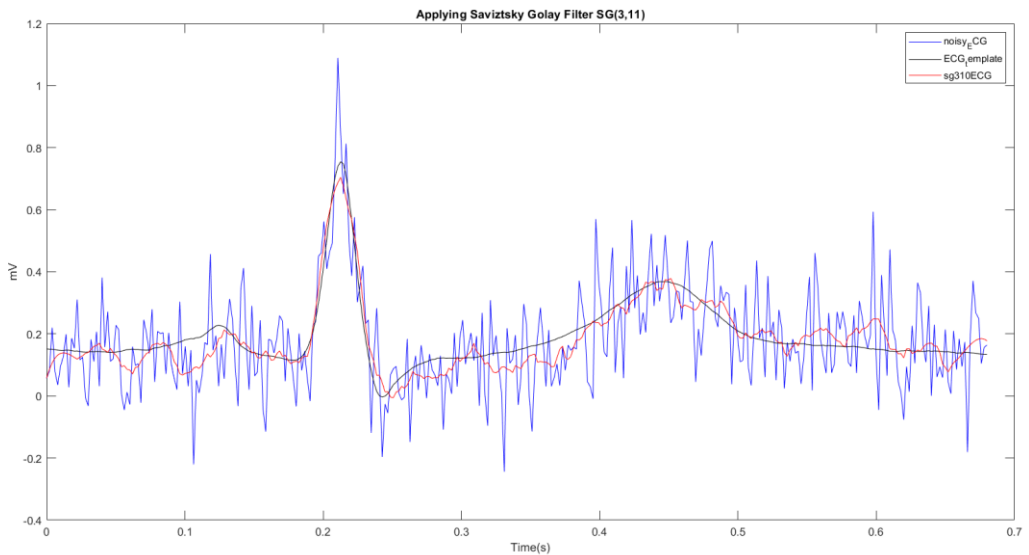


Figure 11: Applying Savitzky Golay Filter (N,L)

By applying Savitzky-Golay filter is also smoothened the signal by suppressing the high frequency noises in the noisy ECG signal.

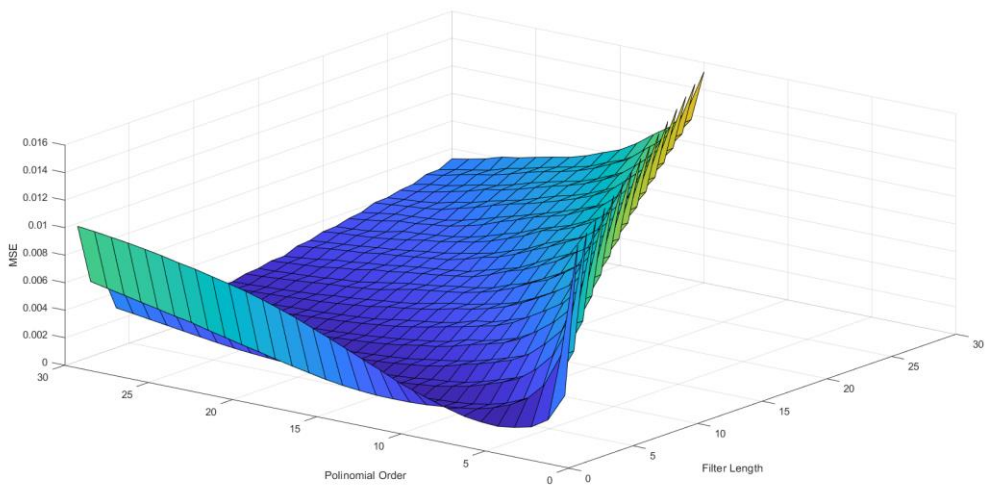


Figure 12: Error vs Order of Savitzsky Golay Filters

Observed Optimum Polynomial Order(N) = 4

Observed Optimum Length of the Window (L) = 17

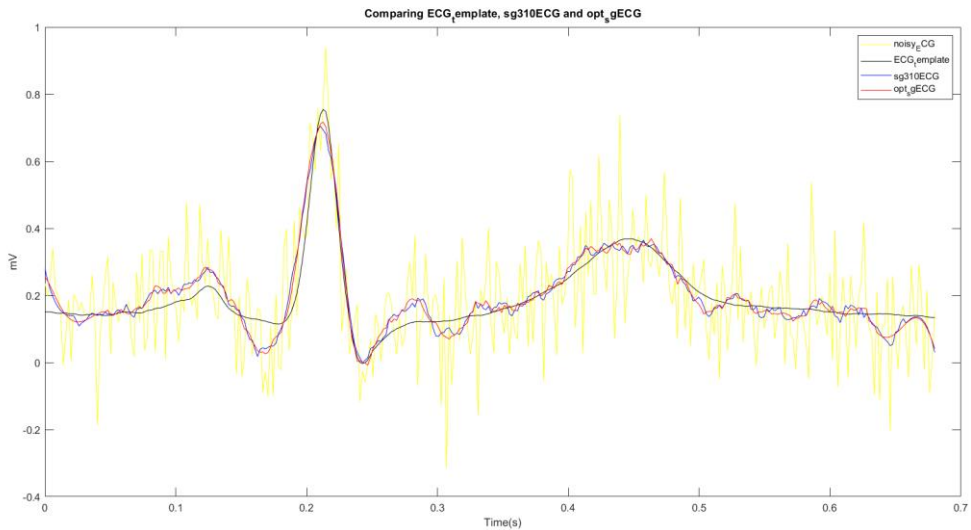


Figure 13: Comparing ECG_template, sg310ECG and opt_sgECG

The optimum SG filter is able to maintain lesser MSE, more smoothenes the signal, higher detection of the peaks than the SG(3,10) filter.

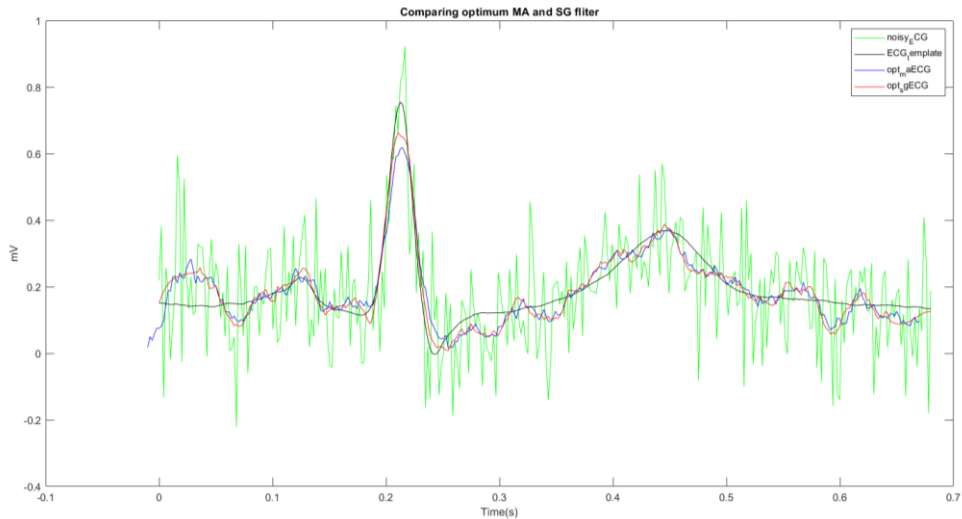


Figure 14: Comparing optimum MA and SG filter

Time elapsed for optimum MA Filter = 0.000110 seconds.

Time elapsed for optimum SG Filter = 0.003004 seconds.

Both filters smoothen the noisy ECG signal by removing high frequency components while Savitzky-Golay filter has more smoothen effect. According to the time analysis data, Moving Average Filter is computationally more efficient since it is ~27 faster than the Savitzky-Golay filter.

2. Ensemble Averaging

2.1. Signal with multiple measurements

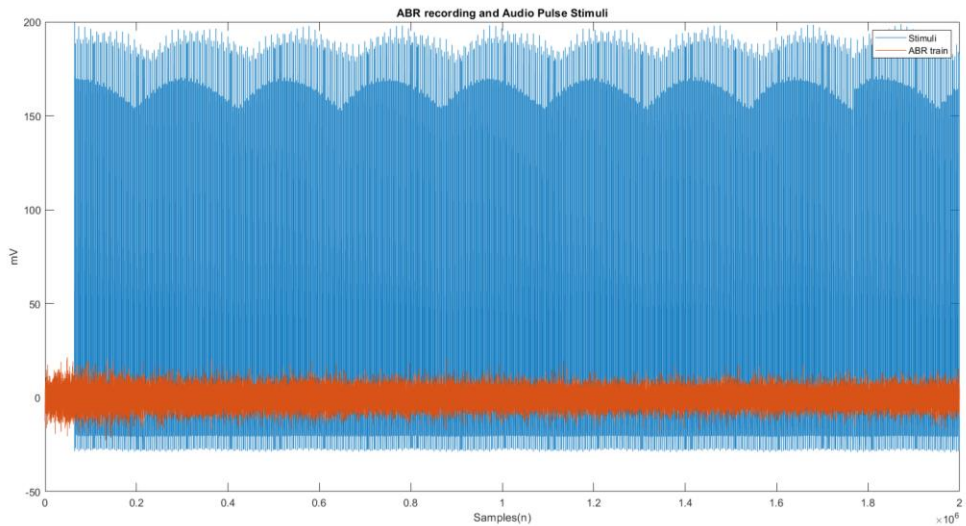


Figure 15: ABR recording and Audio Pulse Stimuli

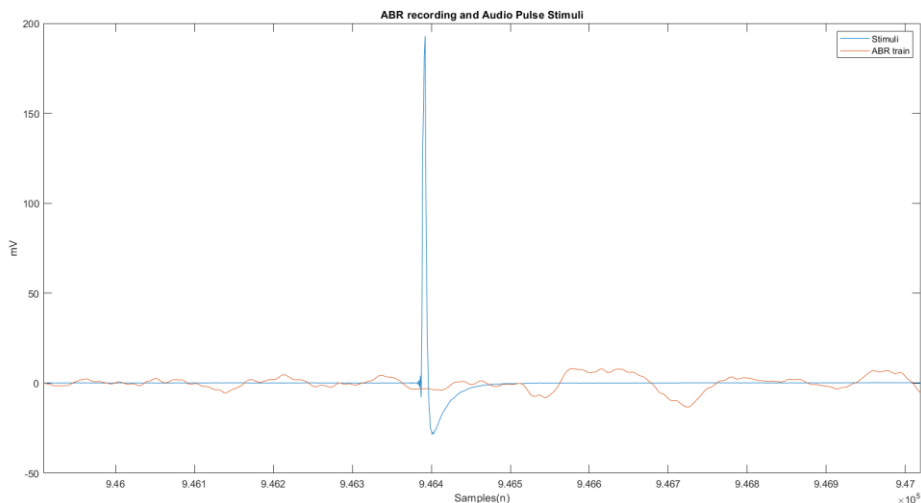


Figure 16: Zoomed Auditory Stimuli and EEG recording

When we investigate a zoomed sample, we can observe and distinguish the auditory stimulus and the ABR EEG recording.

To obtain the ensemble average, the stimulus was selected using a threshold and using those stimulus data points, a sample window of -80 to 399 chosen from each highest stimulus data points. After that, using the extracted samples, ensemble average is calculated and plotted. The plotted graph looks like in Figure 17.

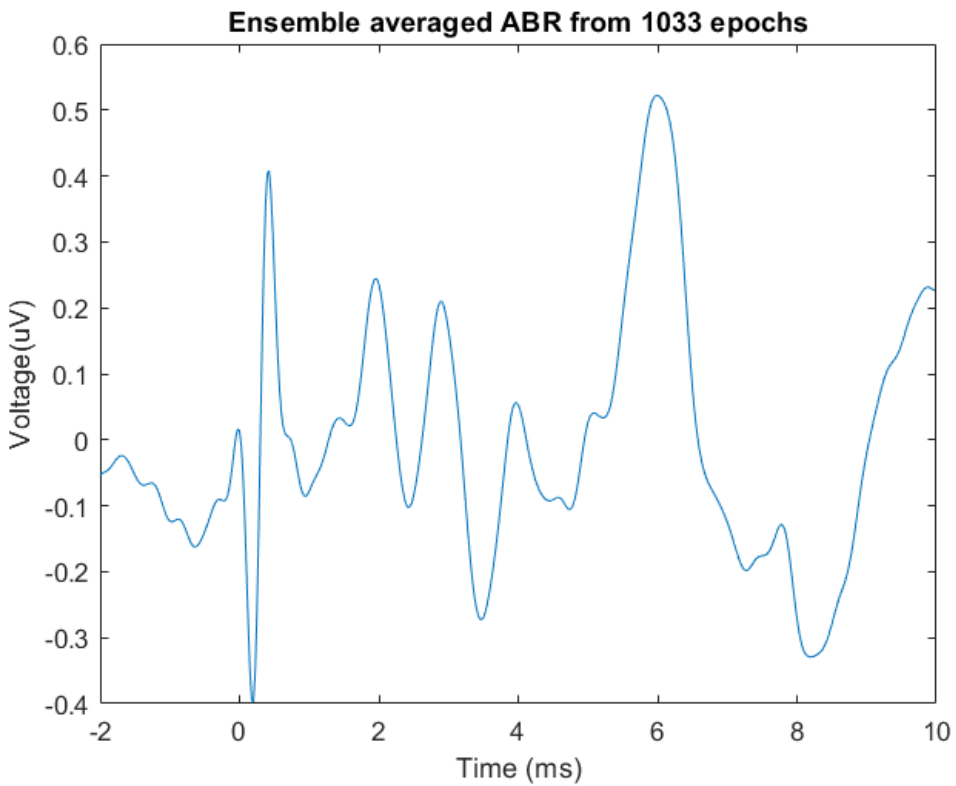


Figure 17: Ensemble averaged ABR

Improvement of the SNR

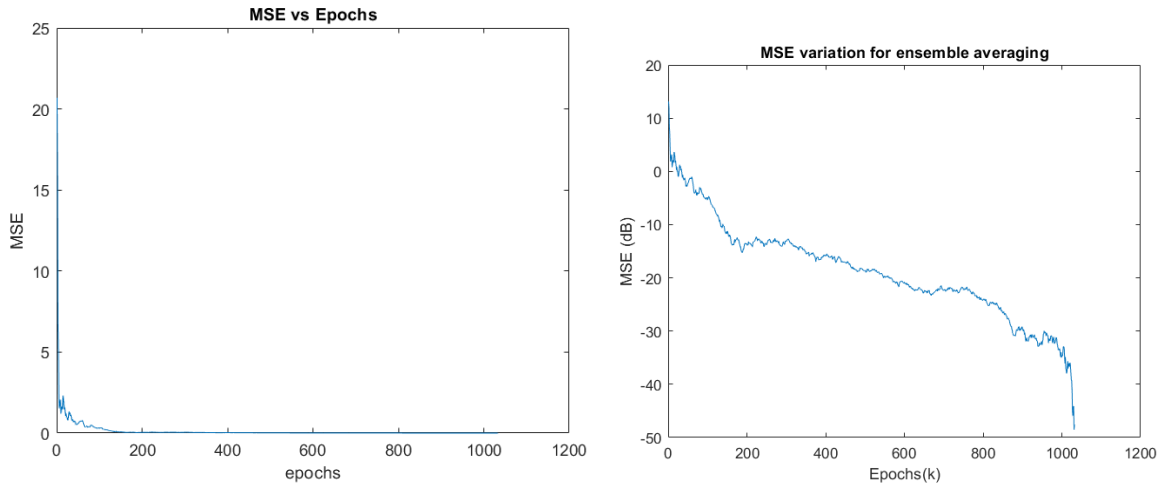


Figure 18: MSE vs epochs

According to the Figure 18 we can see that the Mean Squared Error is significantly reduced and equal to almost zero in higher number of epochs been used to calculate ensemble average. And it can be clearly visible in the logarithmic scale where graph approach to a large negative value. For a better observation SNR is derived and plotted.

Since we are using k number of epochs to obtain the ensemble average, the total signal can be expressed as,

$$S_k = \sum_{j=1}^k S_j = k S_j$$

Likewise, the random noise of the total signal is equal to the sum of variances of all the signal components.

$$\sigma_k^2 = \sum_{j=1}^k \sigma_j^2 = k \sigma_j^2 \Rightarrow \sigma_k = \sqrt{k} \sigma_j$$

\therefore SNR can be expressed as,

$$SNR_k = \frac{S_k}{\sigma_k} = \frac{k S_j}{\sqrt{k} \sigma_j} = \sqrt{k} \frac{S_j}{\sigma_j} = \sqrt{k} SNR_j$$

This implies that the SNR is proportional to the $\sqrt{\text{number of epochs}}$. And in logarithmic scale we can express this as,

$$SNR_k = \frac{1}{2} 20 \log k + SNR_j = 10 \log k + SNR_j$$

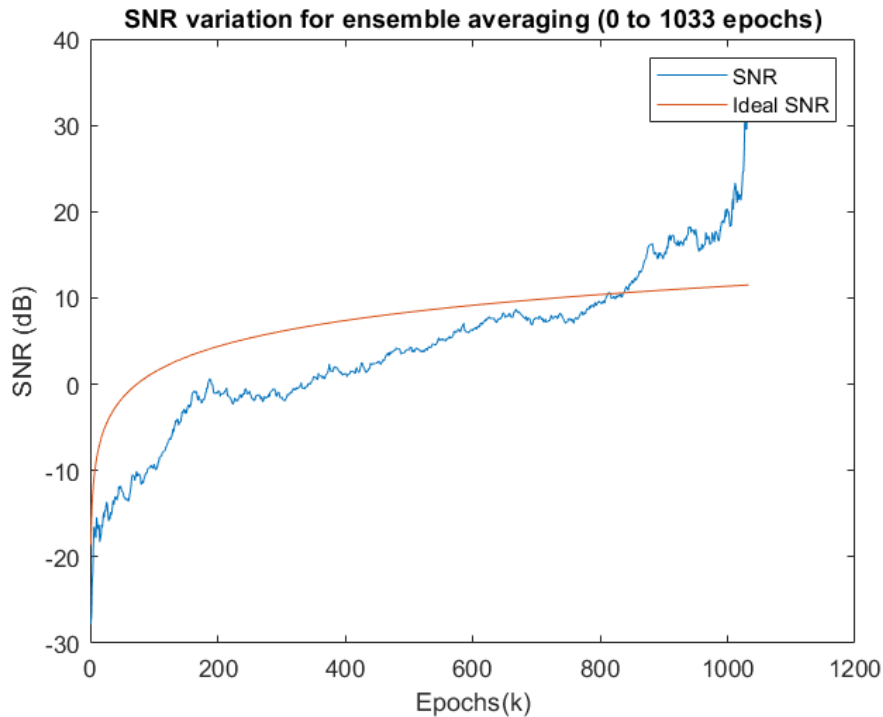


Figure 19: SNR variation vs epochs

2.2. Signal with repetitive patterns

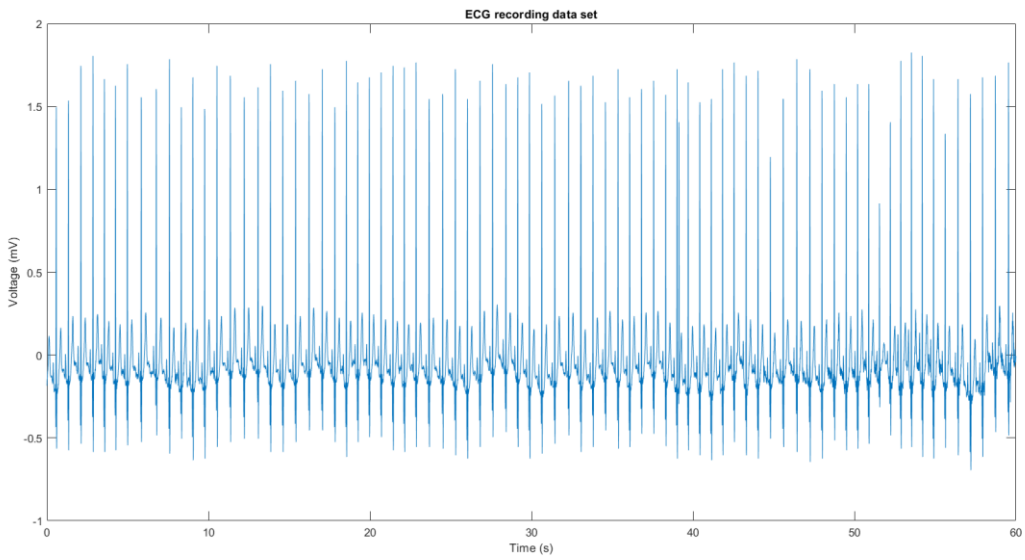


Figure 20: ECG recording data set

Scaled signal is obtained according to a 1.5s time window containing 192 (1.5×128) data samples with 2 ECG pulses.

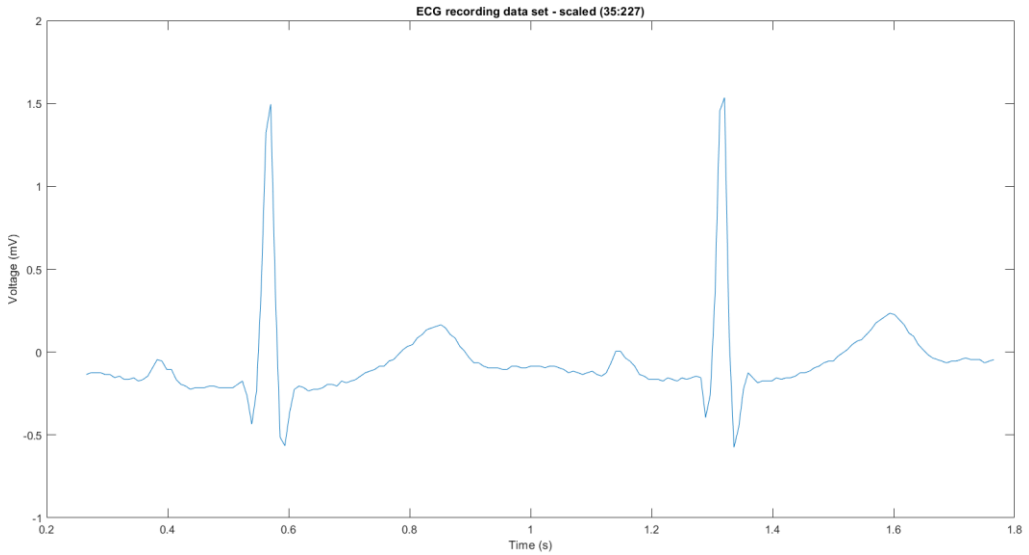


Figure 21: ECG recording data set - scaled

Found the peaks of the data set and chose the 20th peak and extracted the single waveform by taking 0.35 times of the mean pulse time data points before the peak and 0.65 times of the mean pulse time data points after the peak (Since the peak is not at the middle of the pulse).

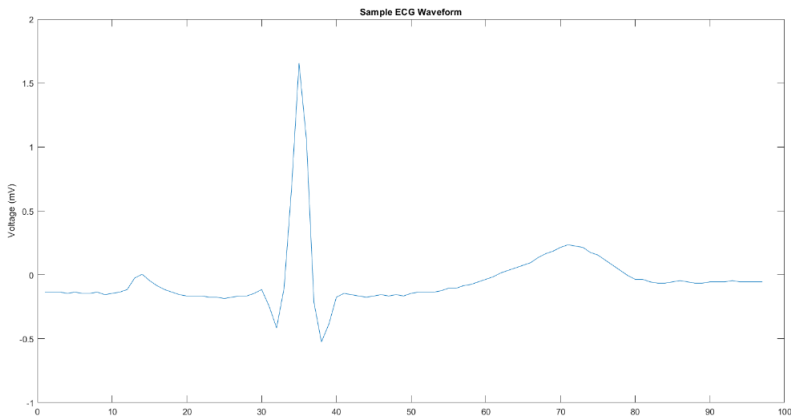


Figure 22: Single ECG Waveform

5dB Gaussian noise is added to the ECG_rec data set

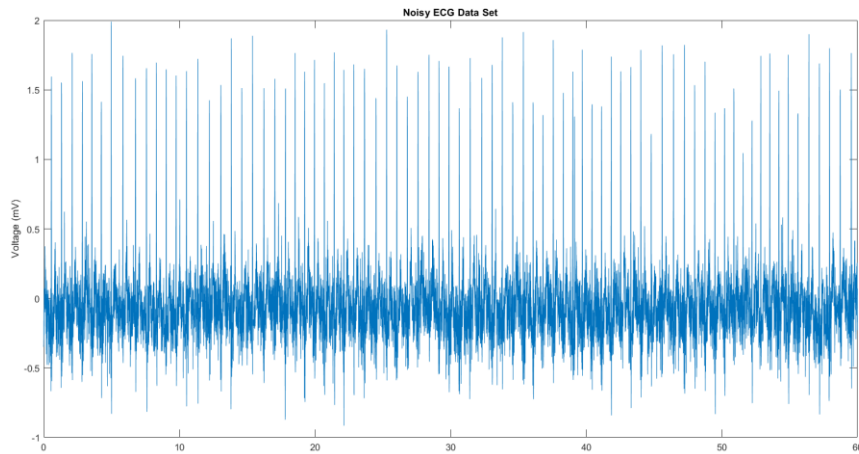


Figure 23: Noisy ECG Dataset

Without using the peak of the QRS complex, here we use cross correlation between the noisy ECG signal and the ECG template, where we move the ECG template along the noisy ECG data and find the points where it gives the highest cross correlation values to obtain the best overlapping positions for the peaks.

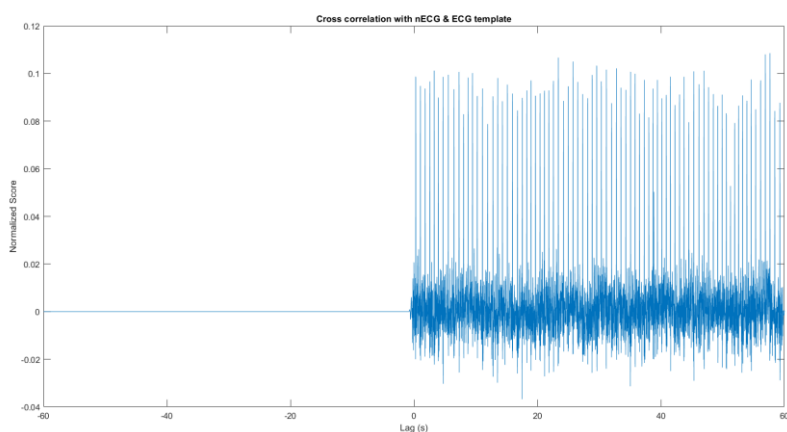


Figure 24: Cross correlation with nECG & ECG template

By looking into the Figure 24, we can define the cross-correlation threshold as **0.08**, to find the pulse starting points.

The SNR of ensemble averaged ECG signal can be shown as,

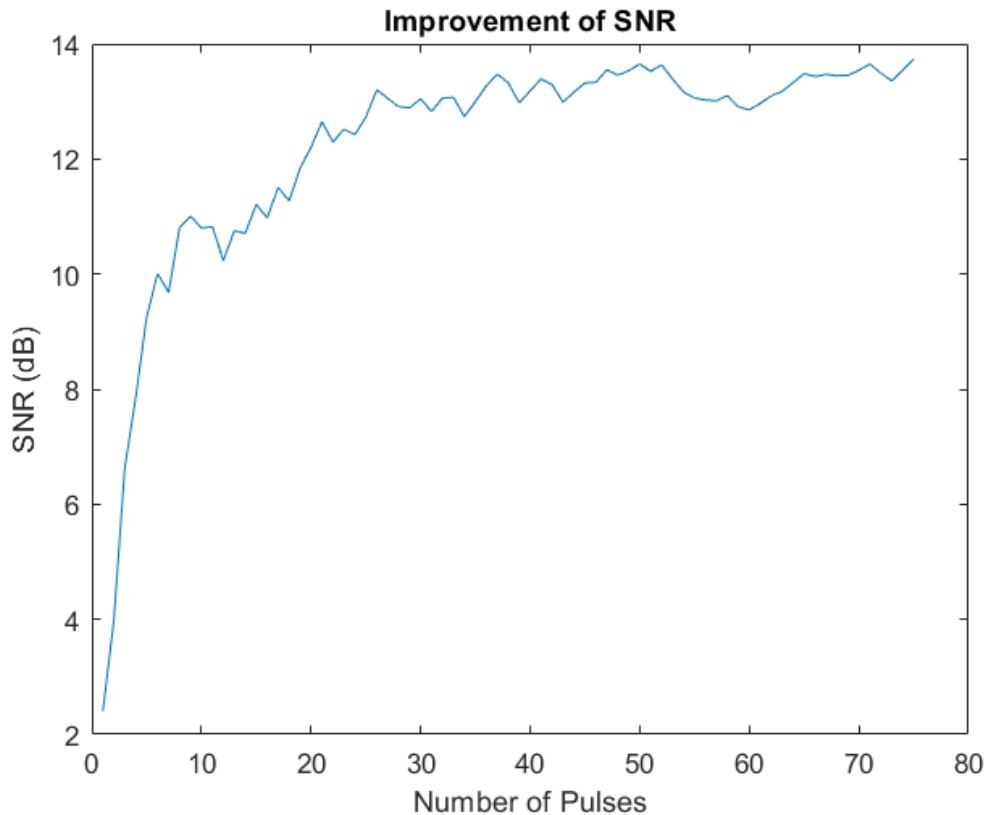


Figure 25: Improvement of SNR

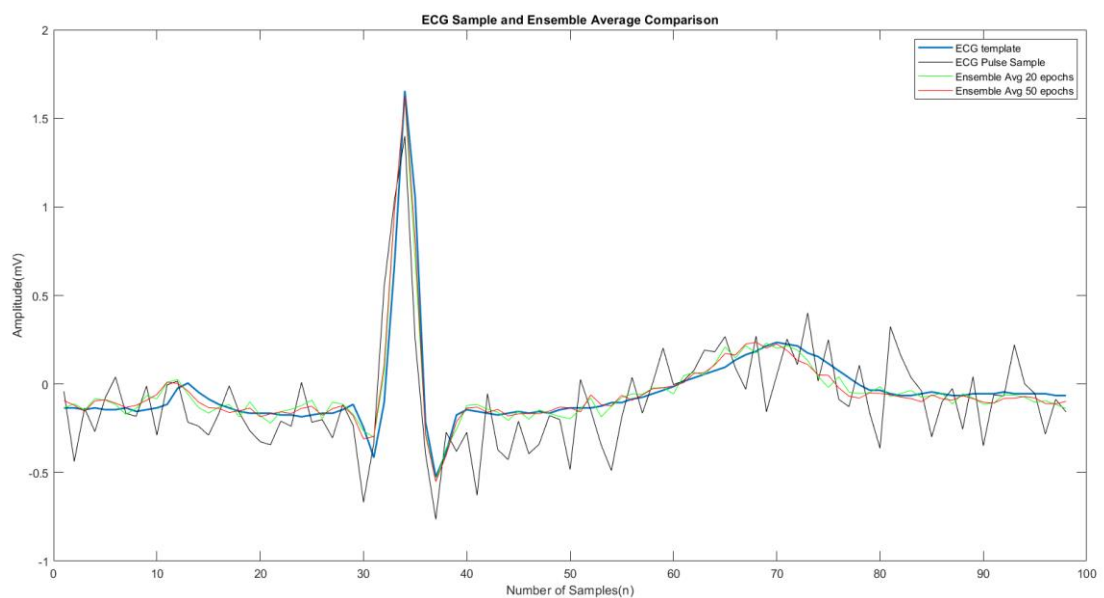


Figure 26: ECG Sample and Ensemble Average Comparison

Figure 26 shows that when increasing the number of epochs in ensemble averaging the ECG waveform become smoother and more likely to the ECG template. As well, when looking into the Figure 25, SNR is almost same after the 30 number of pulses. So, there won't be any significant difference between ensemble averaged samples with pulses greater than 30.

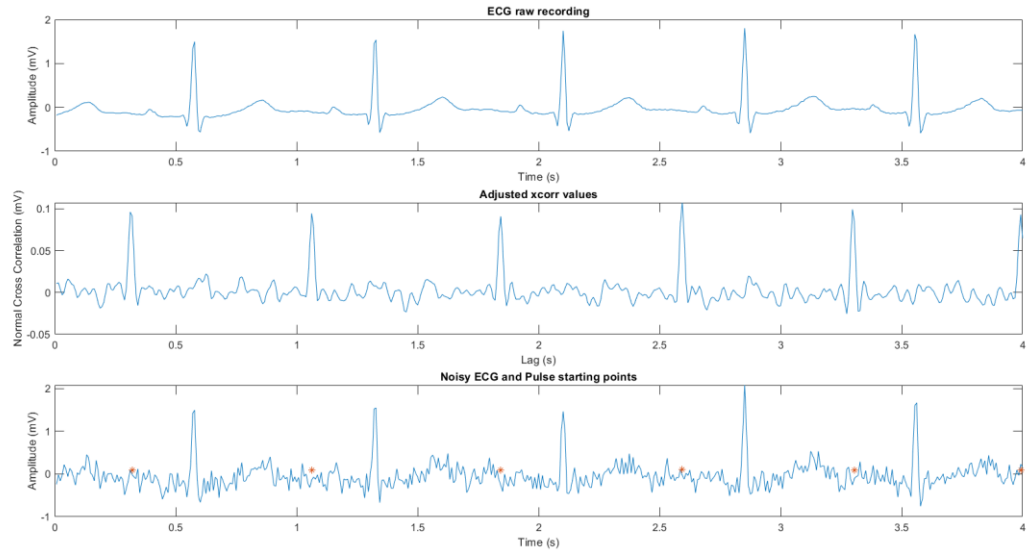


Figure 27: xcorr pulse detection

By looking into the Figure 27, we can see that the higher cross correlation values are detected in pulses starting location and when comparing the 1st and 2nd plots, we can see that all pulses are detected correctly.

Why cross correlation is better over detecting the peak in the QRS complex?

- Time window may vary, different p/t waves
- Abnormal wave rejection

3. FIR derivative filters

3.1. FIR derivative filter properties

Moving average use coefficients to multiply time shifted samples though the coefficients are same or not. Different kinds of FIR filters can be obtained by changing the filter coefficients. One of them is derivative based filter.

The derivative is,

$$y(n) = \frac{d(x(n))}{dt} = \frac{x(n) - x(n-1)}{\delta t}$$

For a signal with T sampling frequency, the equation can be written as,

$$y(n) = \frac{x(n) - x(n-1)}{T}$$

After, converting this to frequency domain, we can obtain the transfer function with filter coefficients $b_0 = 1$, $b_1 = 1$ and $b_k = 0$ for all $k > 1$, And this is a first order filter.

$$H(\omega) = \frac{(1 - z^{-1})}{T}$$

Likewise, we can use central difference equations to implement derivative-based filters where we use the forward and the backward difference.

$$y(n) = \frac{d(x(n))}{dt} = \frac{x(n + \delta t) - x(n - \delta t)}{2\delta t}$$

For a signal with T sampling frequency, the equation can be written as,

$$y(n) = \frac{x(n+1) - x(n-1)}{2T}$$

When we ignore the time shift, the filter output can be re-written as,

$$y(n) = \frac{x(n) - x(n-2)}{2T}$$

And we can show that this represents a transfer function with filter coefficients $b_0 = 1$, $b_1 = 0$, $b_2 = 1$ and $b_k = 0$ for all $k > 1$.

$$H(\omega) = \frac{(1 - z^{-2})}{2T}$$

Let's compare the filter characteristics of the above derived filters,

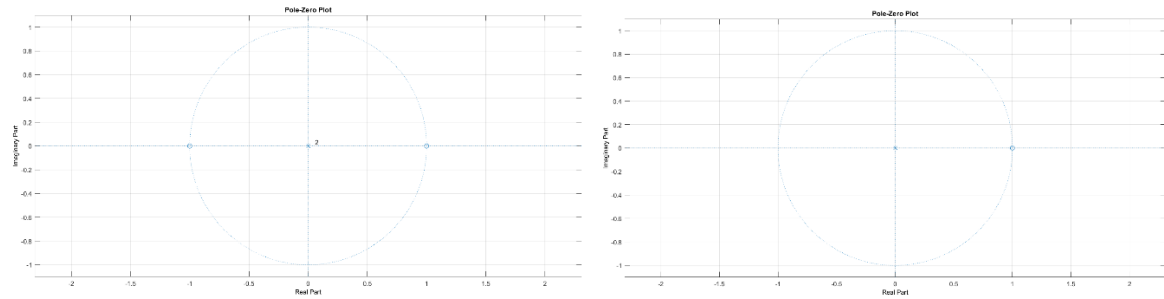


Figure 28: Pole -Zero Plots of First Order Derivative and 3-point Central Difference Filters

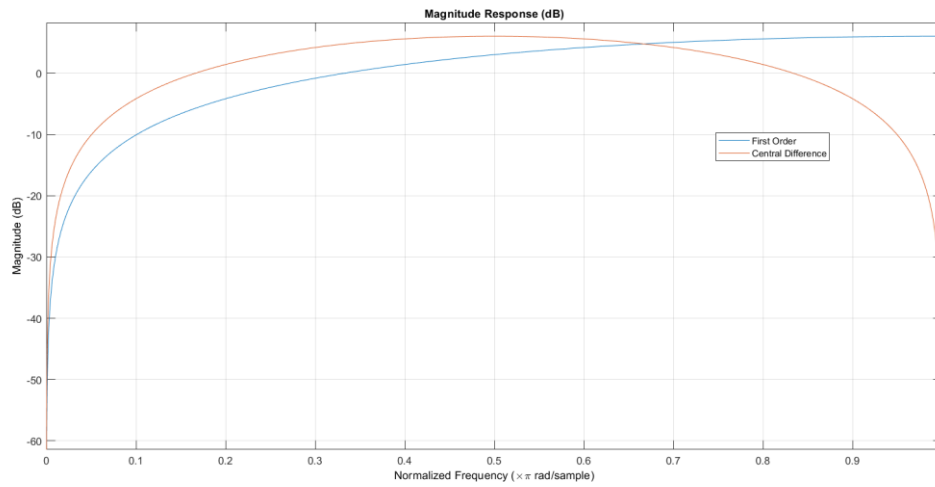


Figure 29: Magnitude Response - Logarithmic Scale

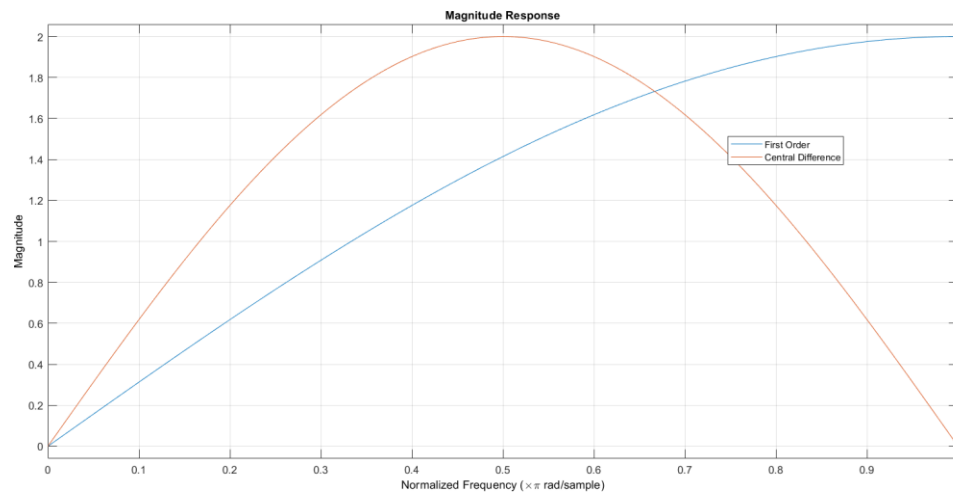


Figure 30: Magnitude Response - Linear Scale

As in the Figure 30, there is an amplification in the pass band frequency where Gain is greater than 1 which may lead to distortions in the passband.

To compensate that effect, we can use a scaling factor to prevent the Magnitude response being exceeding 1. We can define the scaling factor by finding the maximum gain and setting it to 1.

$$\text{Scaling factor } (G) = \frac{1}{|H(\omega)|_{max}}$$

For First order Filter,

$$H(\omega) = \frac{(1 - z^{-1})}{T} = \frac{|z - 1|}{T|z|} = \frac{|z - 1|}{T} \Rightarrow |H(\omega)|_{max} = \frac{2}{T} ; \text{when } z = -1$$

$$\therefore G = \frac{T}{2} \Rightarrow y(n) = \frac{1}{2} [x(n) - x(n - 1)]$$

For Central Difference Derivative Filter,

$$H(\omega) = \frac{(1 - z^{-2})}{2T} = \frac{|z^2 - 1|}{2T|z^2|} = \frac{|z^2 - 1|}{2T} \Rightarrow |H(\omega)|_{max} = \frac{1}{T} ; \text{when } z = j$$

$$\therefore G = T \Rightarrow y(n) = \frac{1}{2} [x(n) - x(n - 2)]$$

So, for both filters we the gain factor will be 0.5 in order to maintain a unity gain filter.

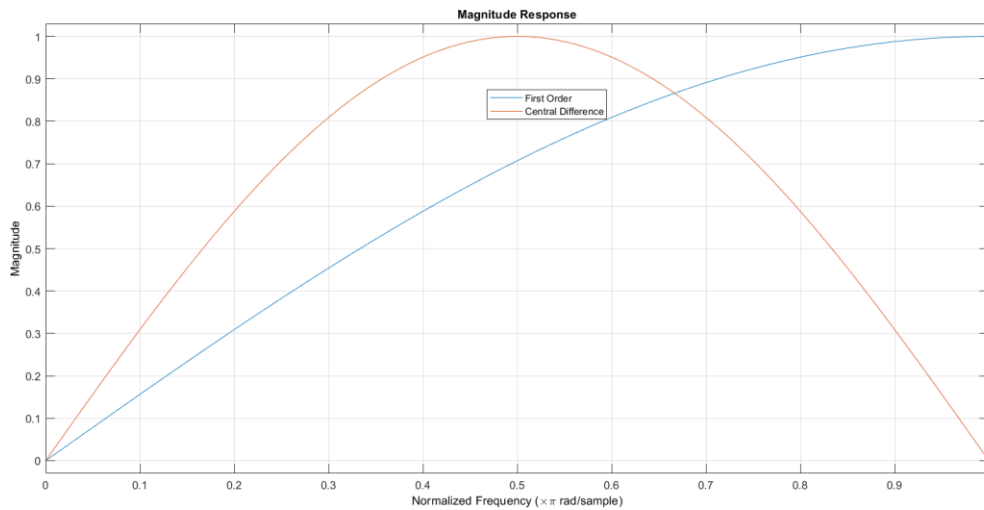


Figure 31: Unity Gain Magnitude Response - Linear Scale

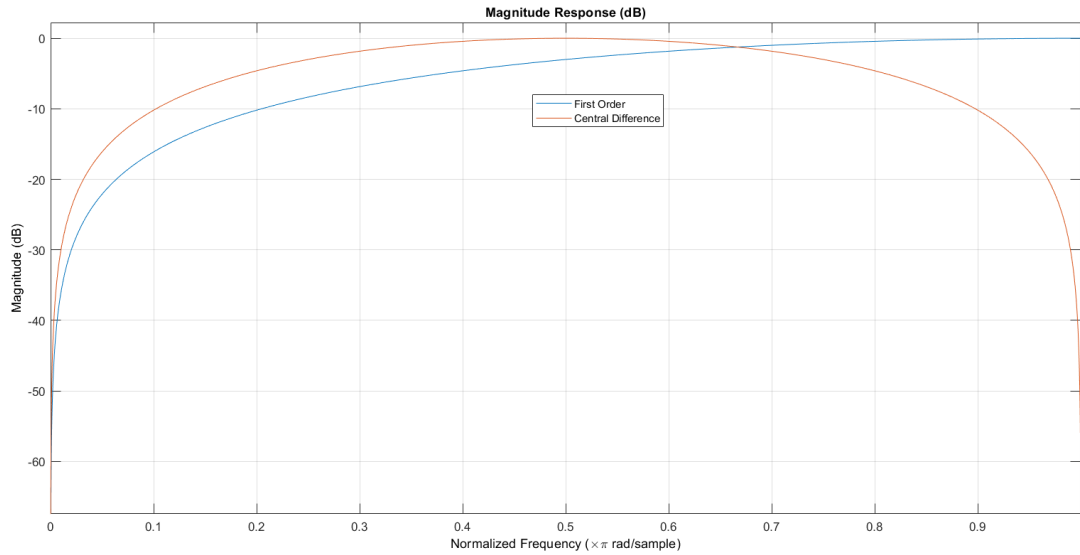


Figure 32: Unity Gain Magnitude Response - Logarithmic Scale

3.2. FIR derivative filter application

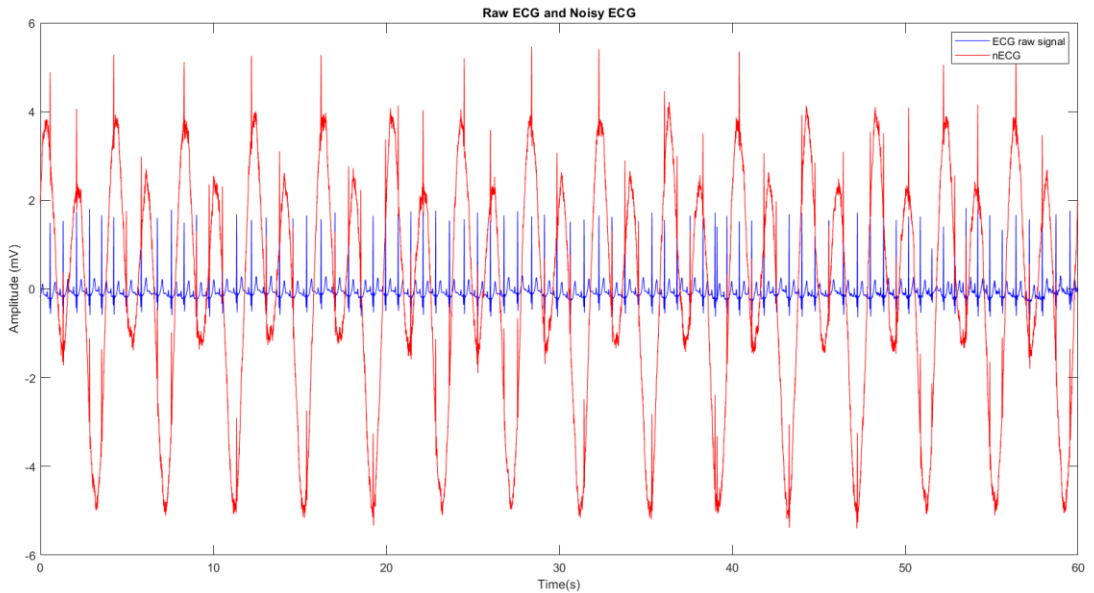


Figure 33: Raw & Noisy ECG

Here we can see that the high frequency noise has been added to the Raw ECG signal.

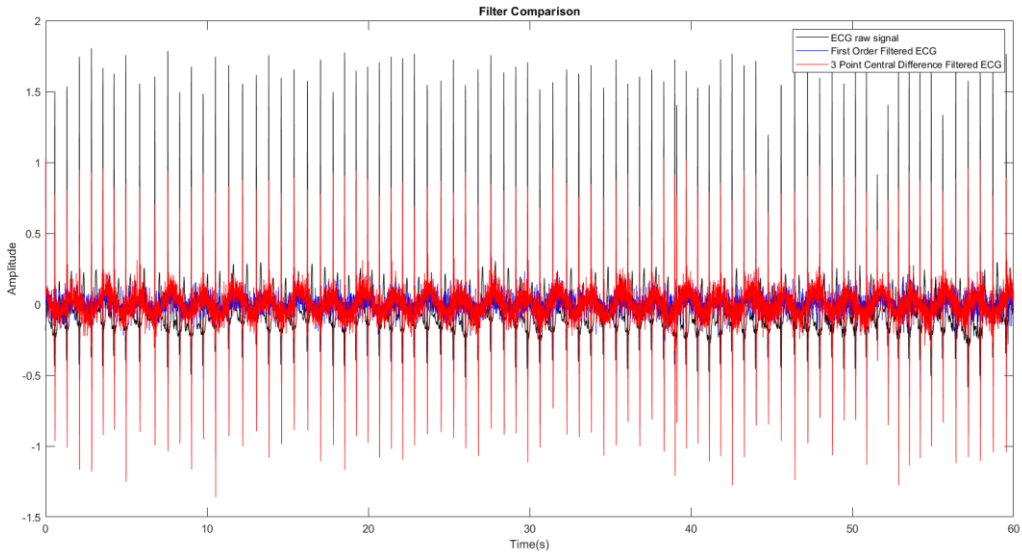


Figure 34: Noisy ECG after applying the Filters

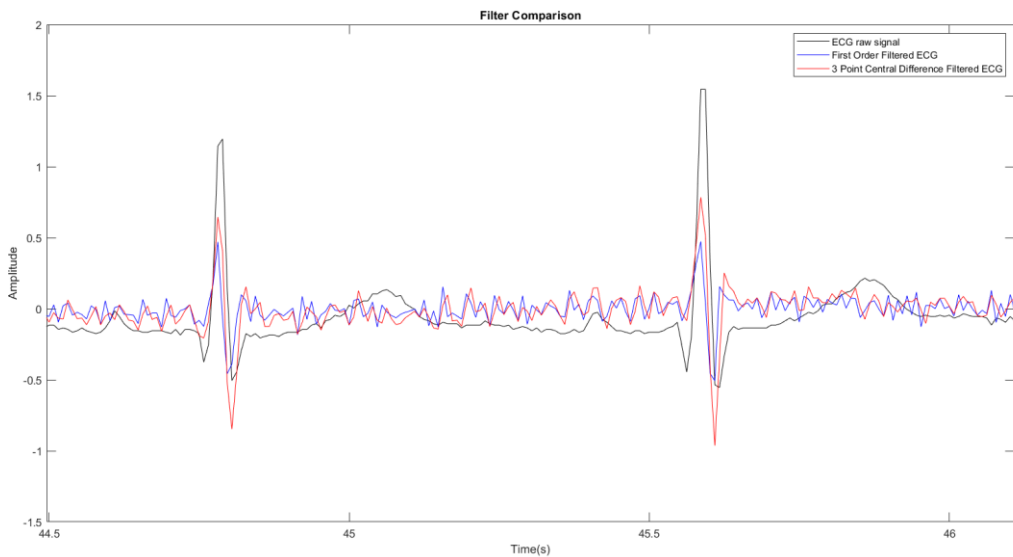


Figure 35: Filter Comparison (Zoomed)

When looking into the Figure 34, we can see that both filters have removed the low frequency EMG noise, but high frequency components are still visible in the signal. Which means that the Filters are unable to remove the high frequency noise. When comparing the filter effect of both filters, the first order filter can attenuate more noise than the 3-point central difference derivative filter. And the first order filter has averaged the R complex peak more than the other filter.

4. Designing FIR filters using windows

4.1. Designing FIR filters using windows

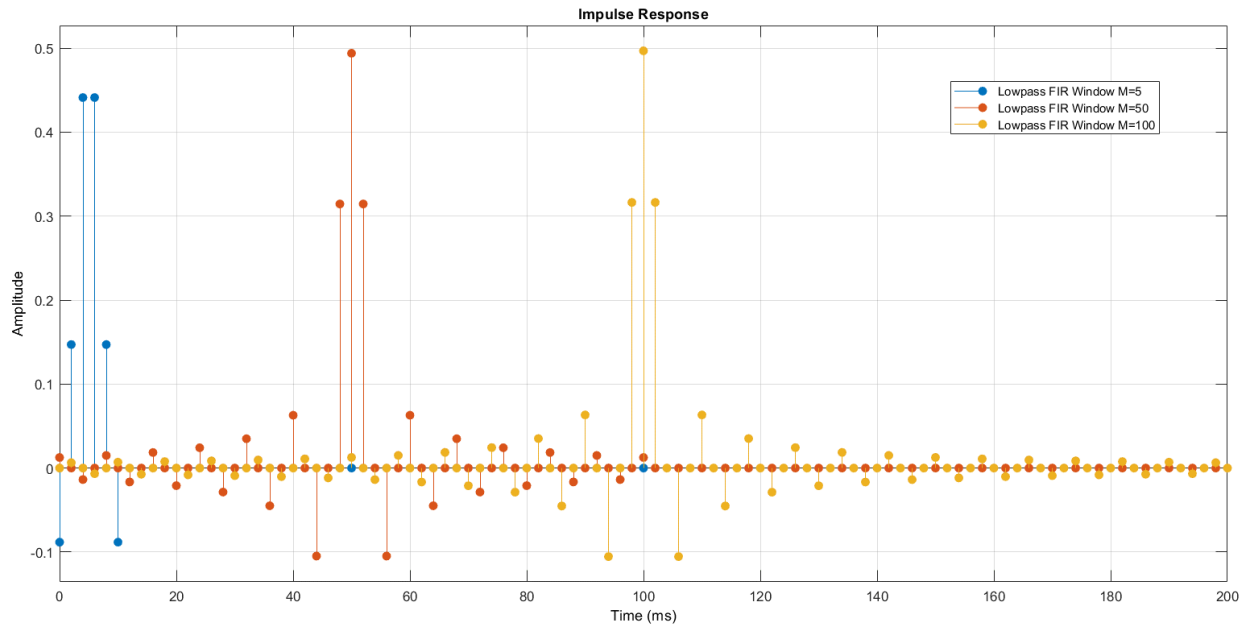


Figure 36: Impulse Response of M=5,50,100 Filters

Designing FIR filters in the window method is normally windowing an ideal filter, $h(n)$ using a window function $w(n)$. This leads to a finite approximation of the ideal filter. A FIR filter designed in window method approaches the ideal filter with increasing window length of M .

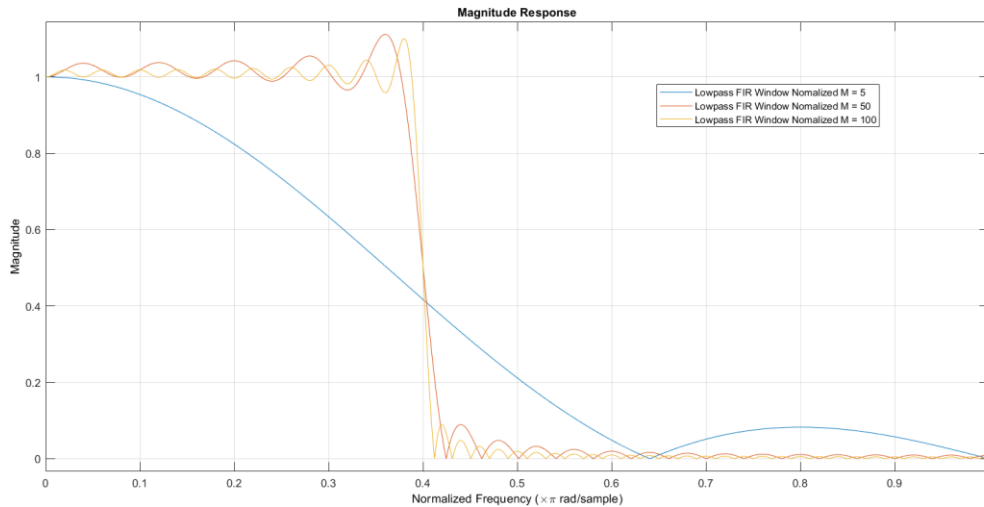


Figure 37: Magnitude Response of LP Filter using Rectangular Window M=5,50,100

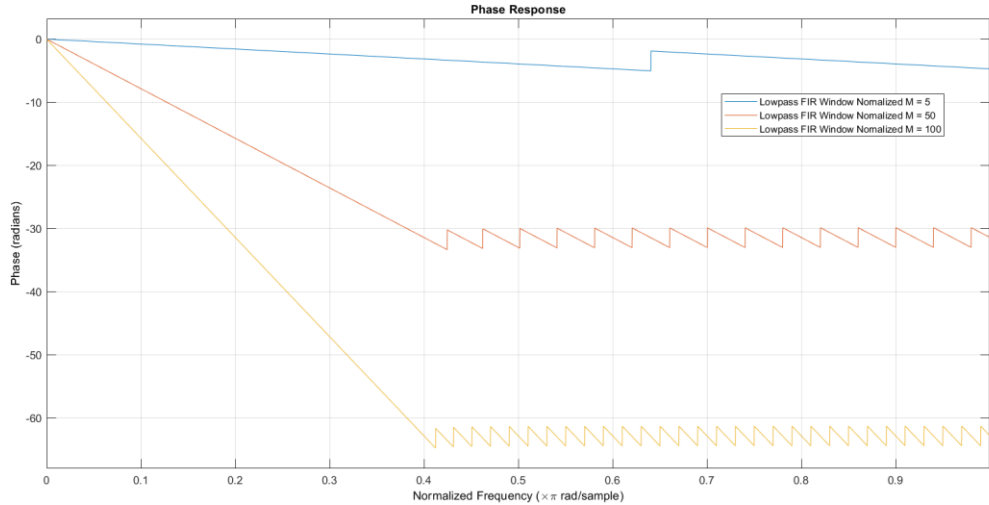


Figure 38: Phase Response of LP Filter using Rectangular Window M=5,50,100

Figure 37, The Magnitude Response Plot, shows that when the order of the window function increases, the filters have sharper cut-off, Narrowed transition bands, higher attenuation at the stop bands and reduced ripples in the pass band.

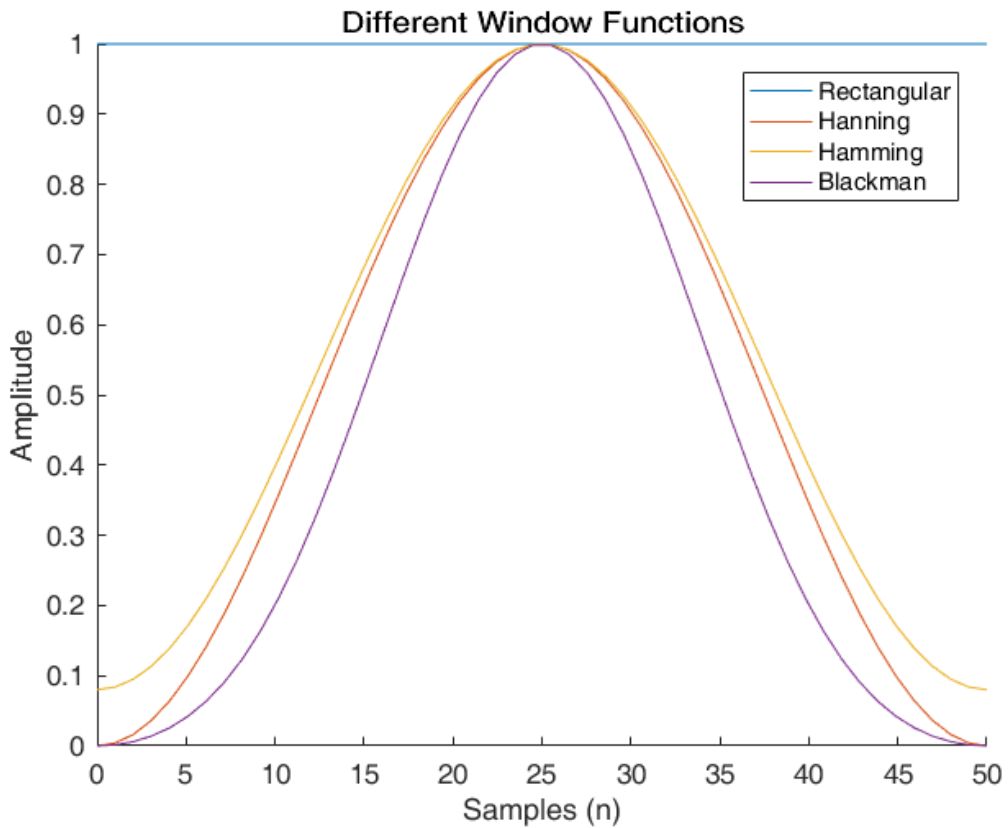


Figure 39: Morphology of Rectangular, Hanning, Hamming and Blackman Filters

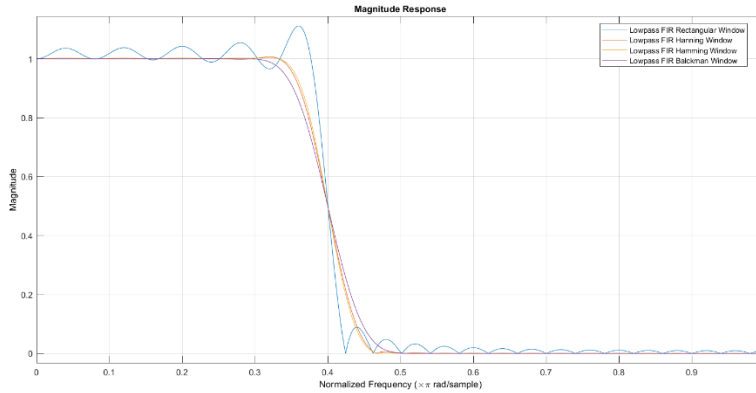


Figure 40: Logarithmic Magnitude Response of Rectangular, Hanning, Hamming and Blackman Filters

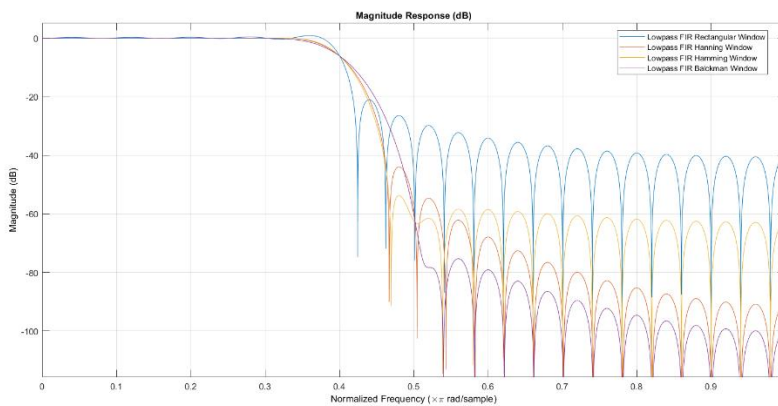


Figure 41: Linear Magnitude Response of Rectangular, Hanning, Hamming and Blackman Filters

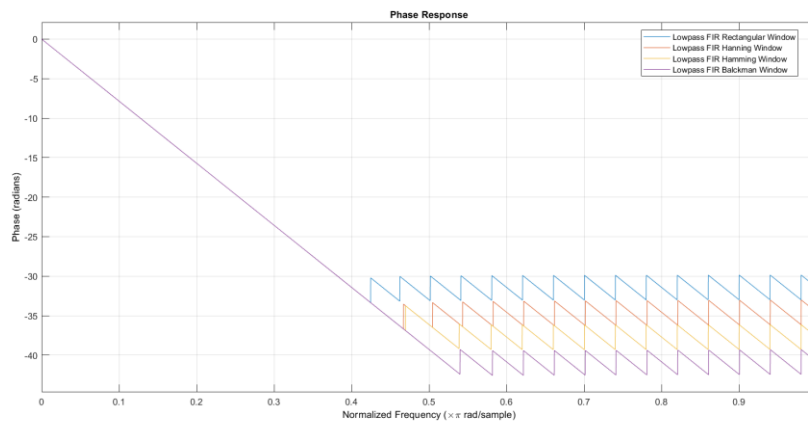


Figure 42: Phase Response of Rectangular, Hanning, Hamming and Blackman Filters

The rectangular window has a rectangular shape where it has sharp transitions at $n = 0$ and $n = M$. Other Hanning, Hamming and Blackman window functions are symmetrical, and bell shaped where transition to 0 to 1 over number of samples. The result of smoothing can be seen in the Figure 41, the Magnitude Response Plot.

4.2. FIR Filter design and application using the Kaiser window

For a given window length, there is a trade-off between transition width around cut-off frequency and ripple amplitude in the pass band and the stop band. Kaiser window gives a solution to that trade-off by providing another parameter to control the window characteristics. It has a shape parameter β , which is an arbitrary value to be calculated based on passband ripple characteristics.

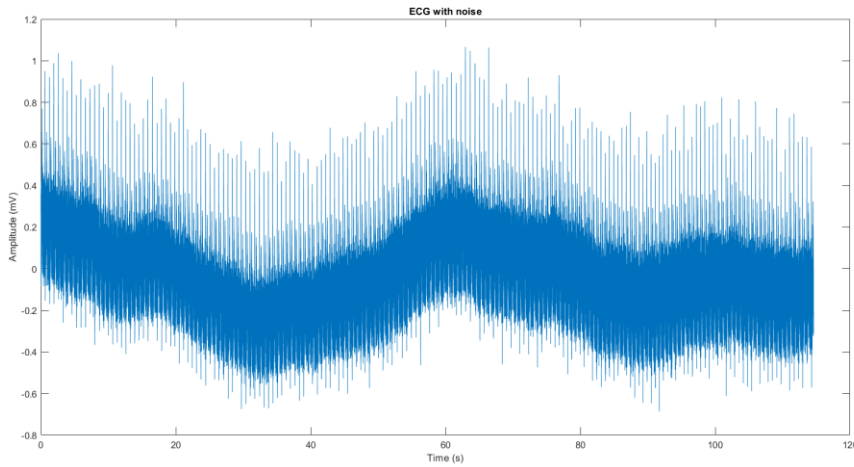


Figure 43: Noisy ECG

This raw data file of ECG signal contains has lot of noise as in the Figure 43. We can clearly see the low frequency component as well as the added high frequency component which has sudden variations.

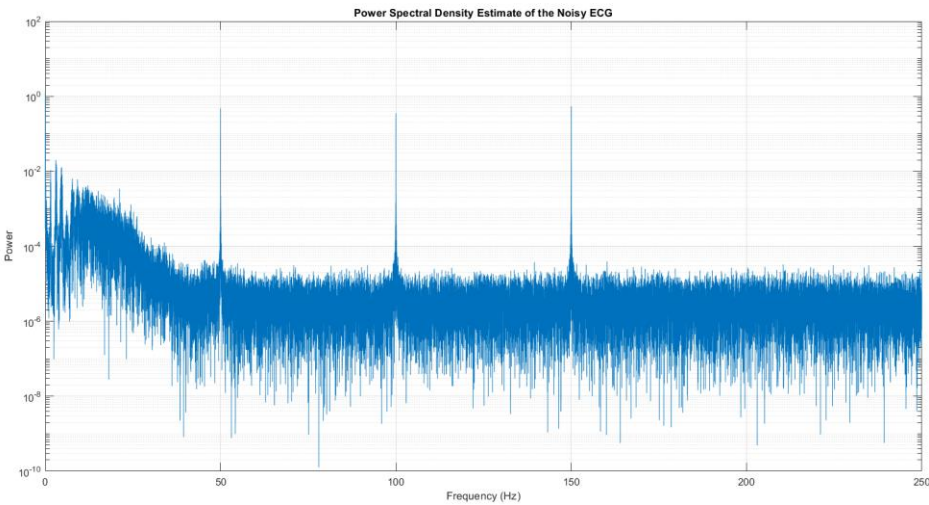


Figure 44: PSD of Noisy ECG

Here we can see that the signal contains lot of high frequency power as well as the power line noise is also visible at 50Hz, 100 Hz and 150 Hz. And random white noise is also visible in the PSD.

	Highpass(Hz)	Lowpass(Hz)
$f_{\text{cut-off}}$	5	125
f_{pass}	7	123
f_{stop}	3	127
δ	0.001	0.001

Comb Filter	
f_{stop1}	50 Hz
f_{stop2}	100 Hz
f_{stop3}	150 Hz

Since, there is a transition width in the filters at the cut-off frequency there are two frequencies defined as f_{pass} and f_{stop} around cut-off frequency. And also the practical filters contains ripples in there pass bands and the stop bands. In Kaiser window, it uses certain parameters to control the ripple effect as well as the other factors.

Following equations are used in implementing the Kaiser window.

$$A = -20 \log \delta$$

$$\Delta\omega = |f_{\text{pass}} - f_{\text{stop}}| \times T ; T = \text{Sampling Period}$$

$$M = \frac{A - 8}{2.285 \Delta\omega}$$

$$\beta = \begin{cases} 0.1102(A - 8.7) & A > 50 \\ 0.5842(A - 21)^{0.4} + 0.07886(A - 21) & 21 \leq A \geq 50 \\ 0 & A < 21 \end{cases}$$

	Highpass	Lowpass
$ f_{\text{pass}} - f_{\text{stop}} $		6 Hz
A		60 dB
M		453
β		5.60476

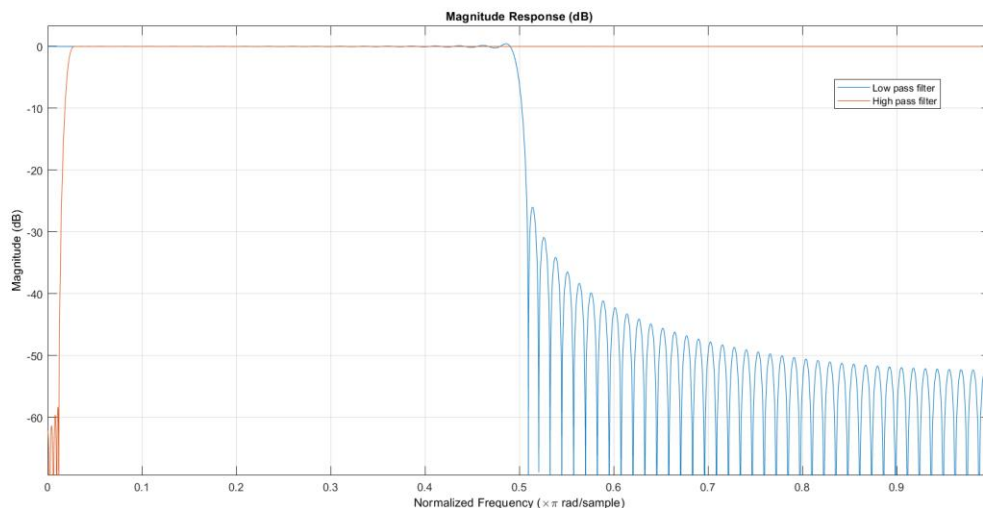


Figure 45: Magnitude Response of LP and HP Filter

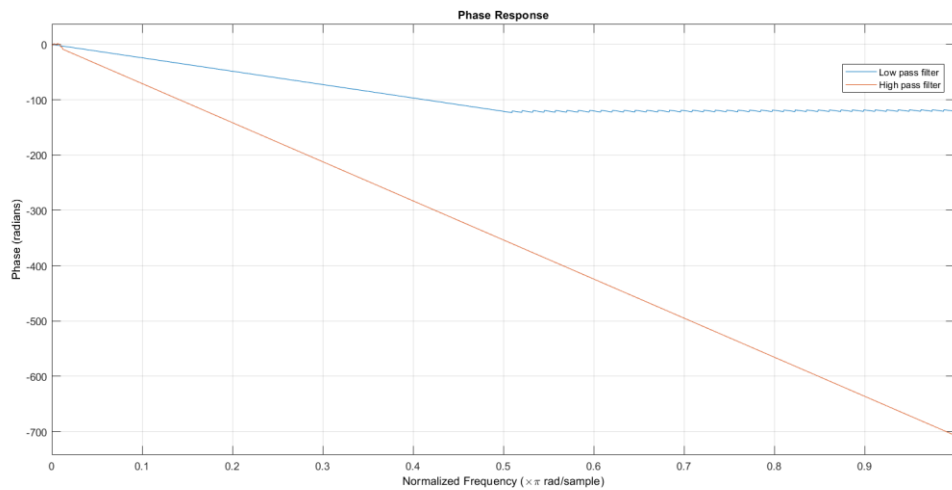


Figure 46: Phase Response of LP and HP Filter

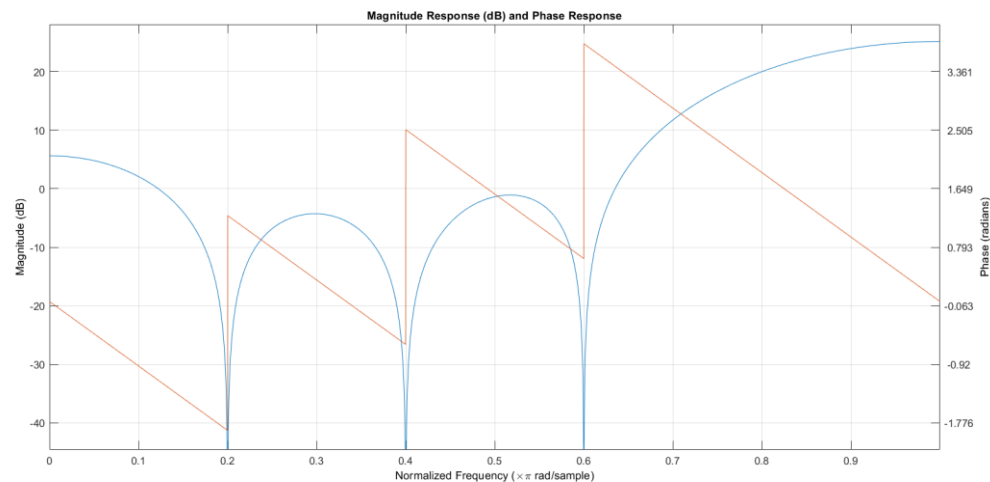


Figure 47: Comb filter

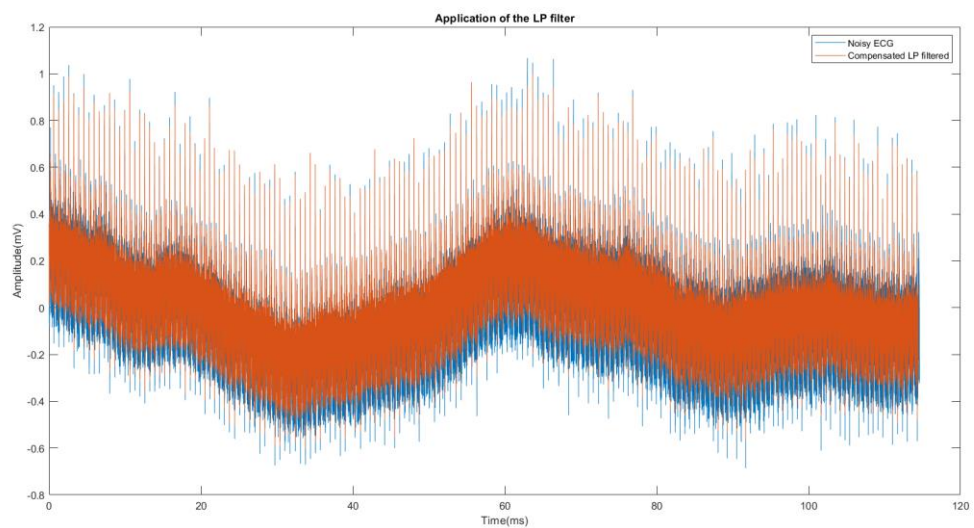


Figure 48: LP Filtered ECG

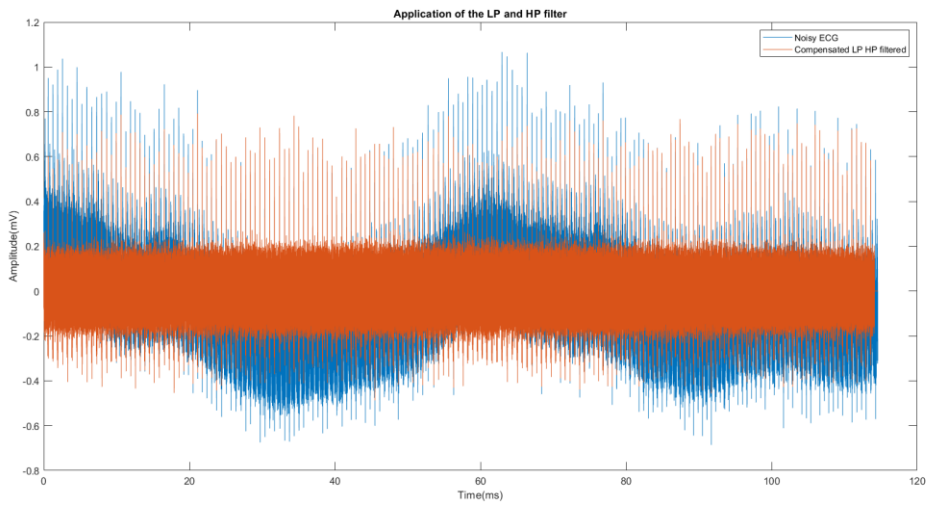


Figure 49: LP & HP Filtered ECG

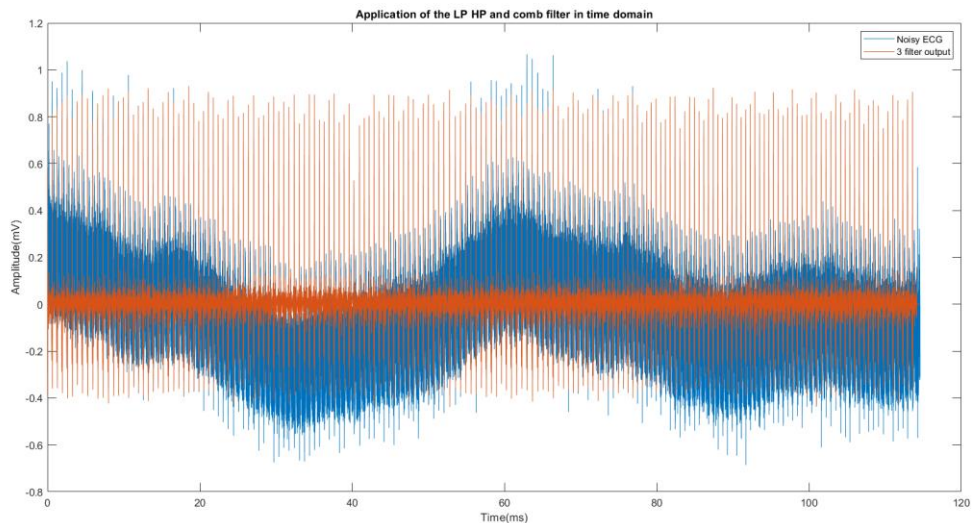


Figure 50: LP, HP and Comb Filtered ECG

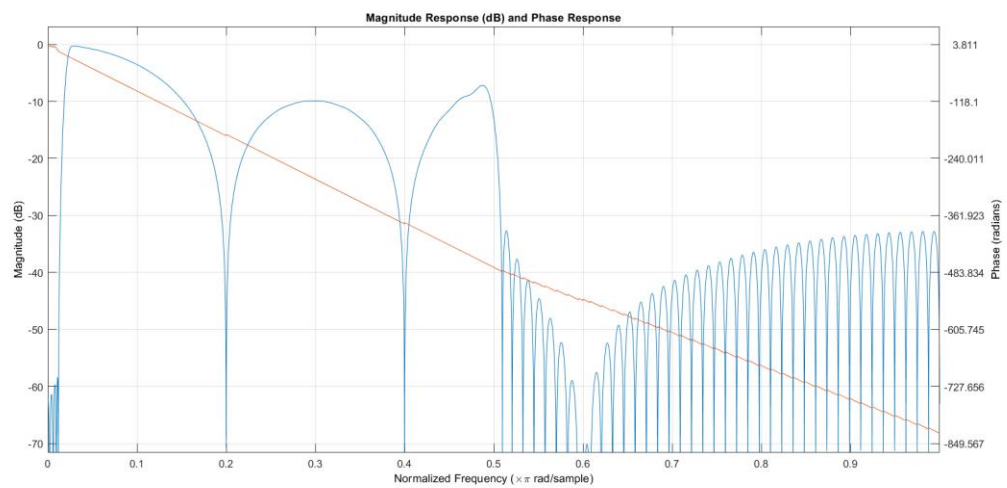


Figure 51: Casacade Filter Magnitude and Phase Response

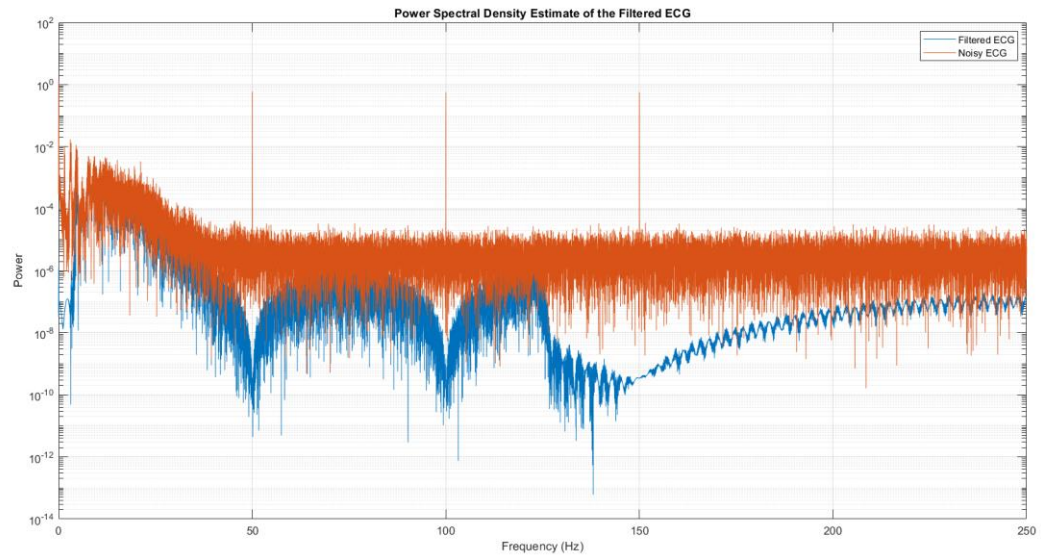


Figure 52: PSD comparison of Filtered Signal and Noisy signal

5. IIR Filter

5.1. Realising IIR filters

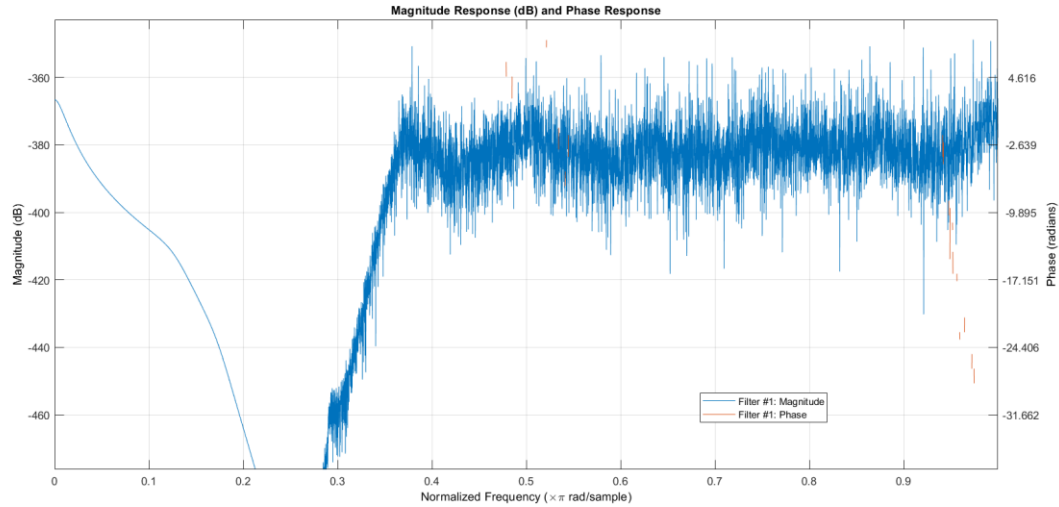


Figure 53: Magnitude and Phase Response of Butterworth LP Filter | M = 453

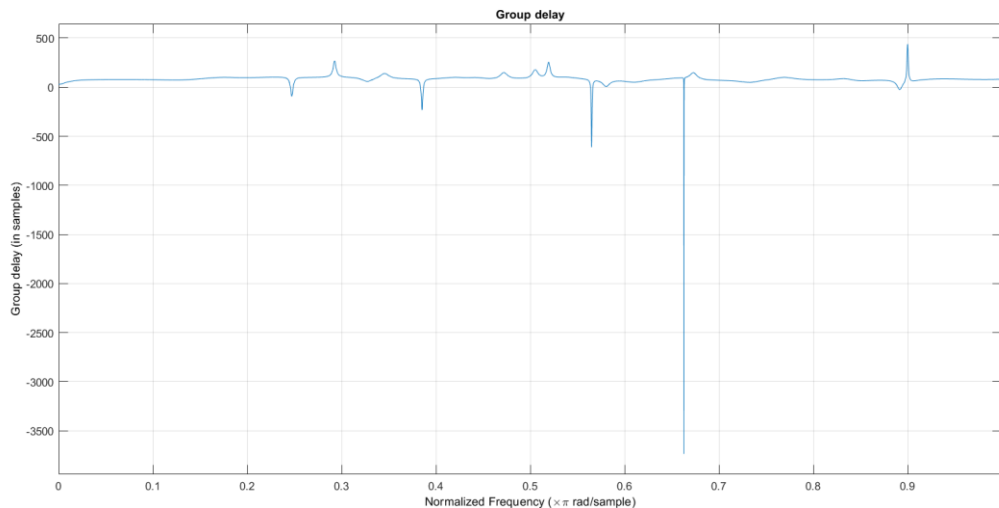


Figure 54: Group Delay Response of Butterworth LP Filter | M = 453

Since, the Butterworth Low pass filter of order 453 in the previous part is not stable, Let's take M as 10 and see the characteristics of those filters.

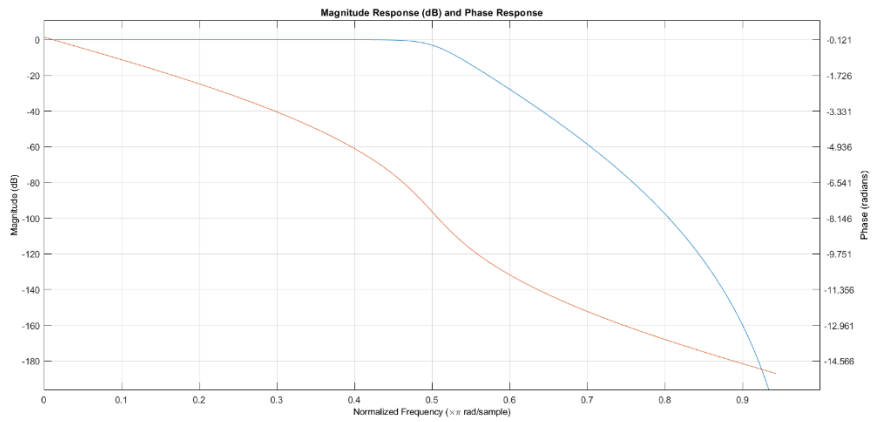


Figure 55: IIR BW LP Filter Magnitude & Phase Response | M = 10

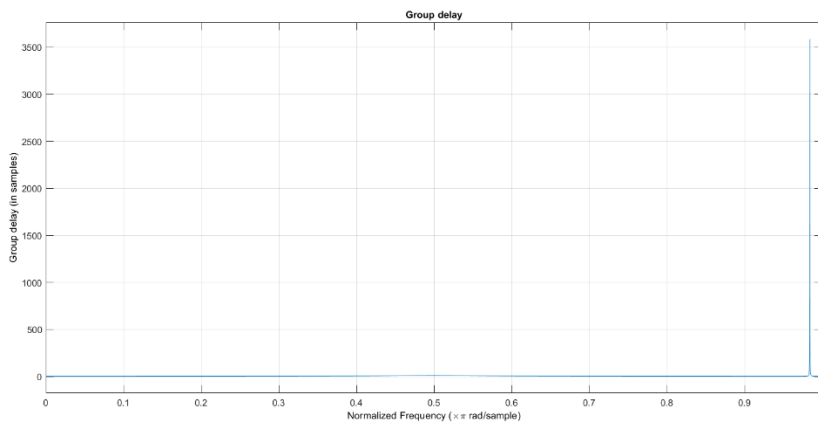


Figure 56: IIR BW LP Filter Group Delay | M = 10

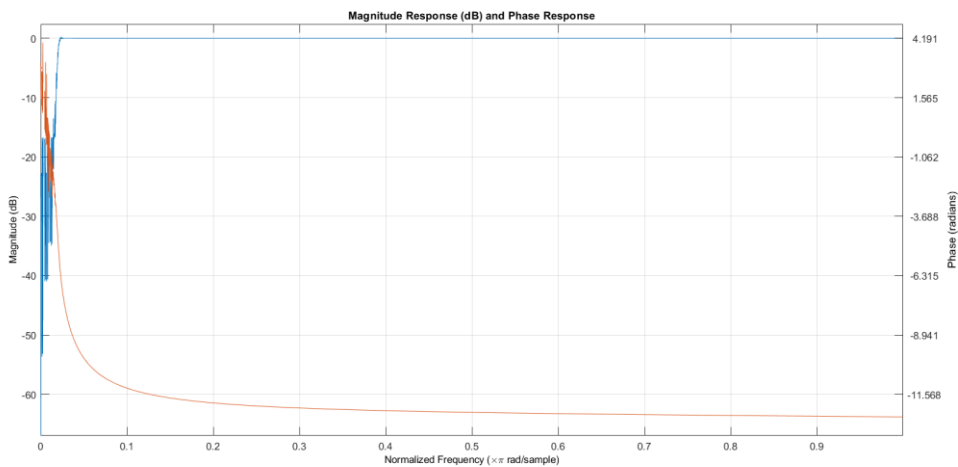


Figure 57: IIR BW HP Filter Magnitude & Phase Response | M = 10

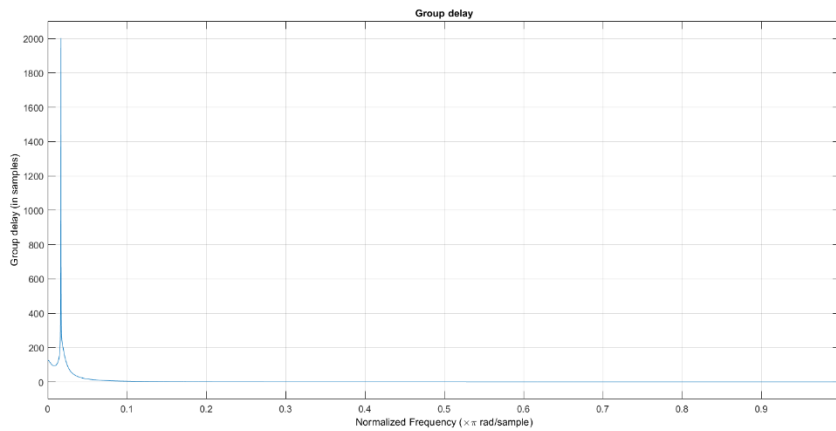


Figure 58: IIR BW HP Filter Group Delay | M = 10

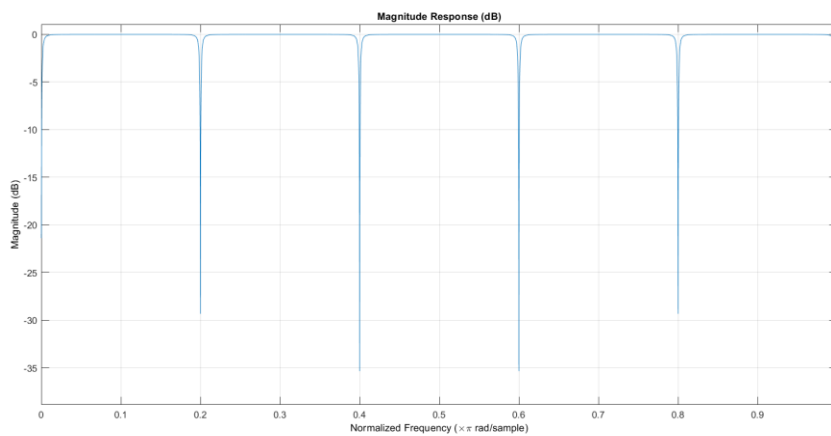


Figure 59: IIR BW Comb Filter Magnitude & Phase Response | M = 10

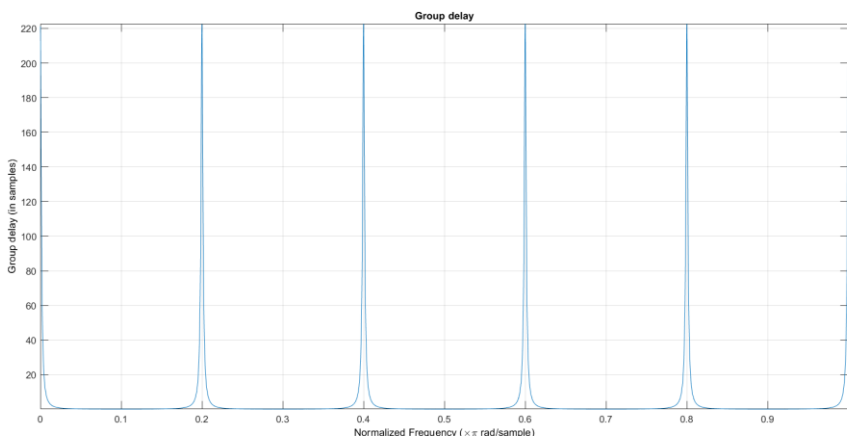


Figure 60: IIR BW Comb Filter Group Delay | M = 10

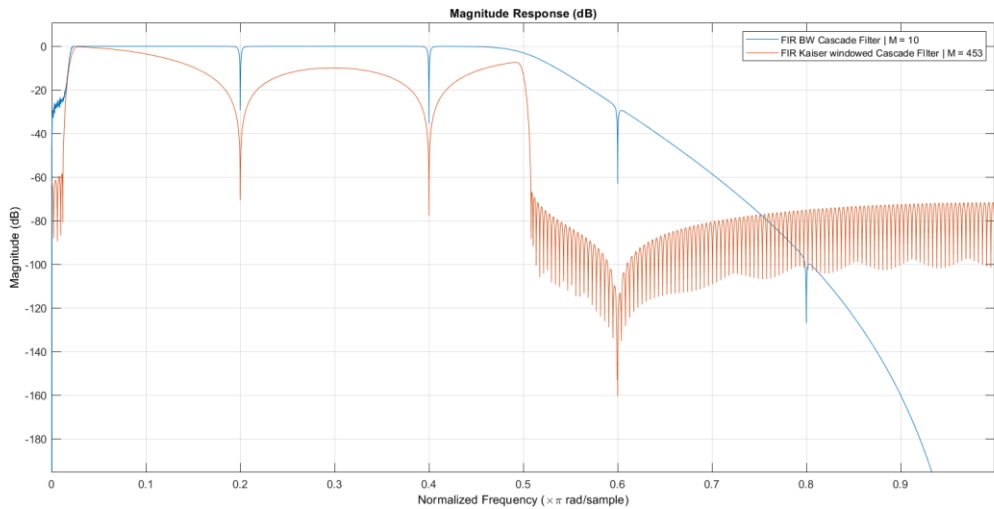


Figure 61: Magnitude Response Comparison

According to the Figure 61, the IIR cascade filter has better magnitude response in the pass band. Also the Notch(comb) filter has a much narrow bandwidth compared to the FIR cascade filter implementation. The stop band attenuation is significantly higher with respect to the FIR magnitude response. And in the IIR, the transition bandwidth is larger than the FIR filter and it depends on the order of the filter.

5.2. Filtering methods using IIR filters

5.2.1. Forward Filtering.

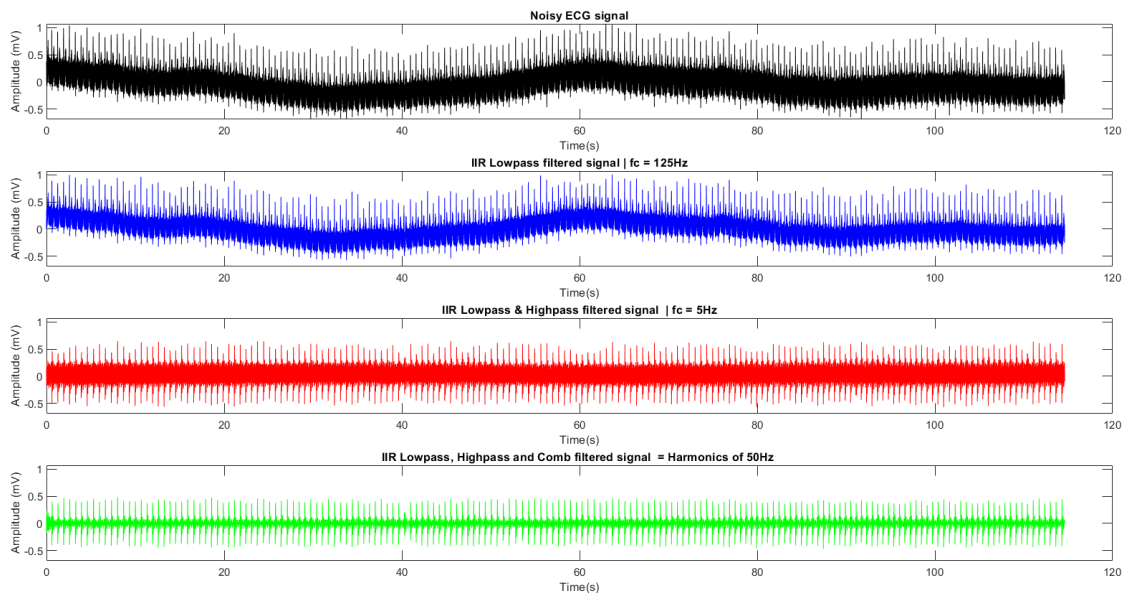


Figure 62: Forward Filtered Signal

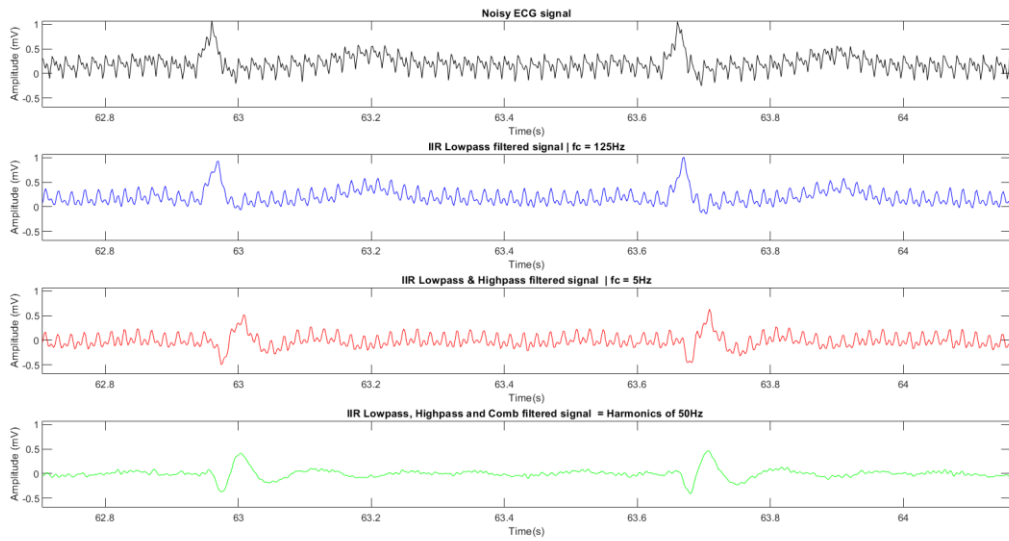


Figure 63: Forward Filtered (Zoomed)

By looking into the 3rd and 4th plots of the Figure 63, we can clearly see the mis alignment of data in the time axis. To over come this draw back forward filtering, forward-backward filtering is used. And it is for compensating the group delay effect shown in forward filtering.

5.2.2. Forward-Backward Filtering

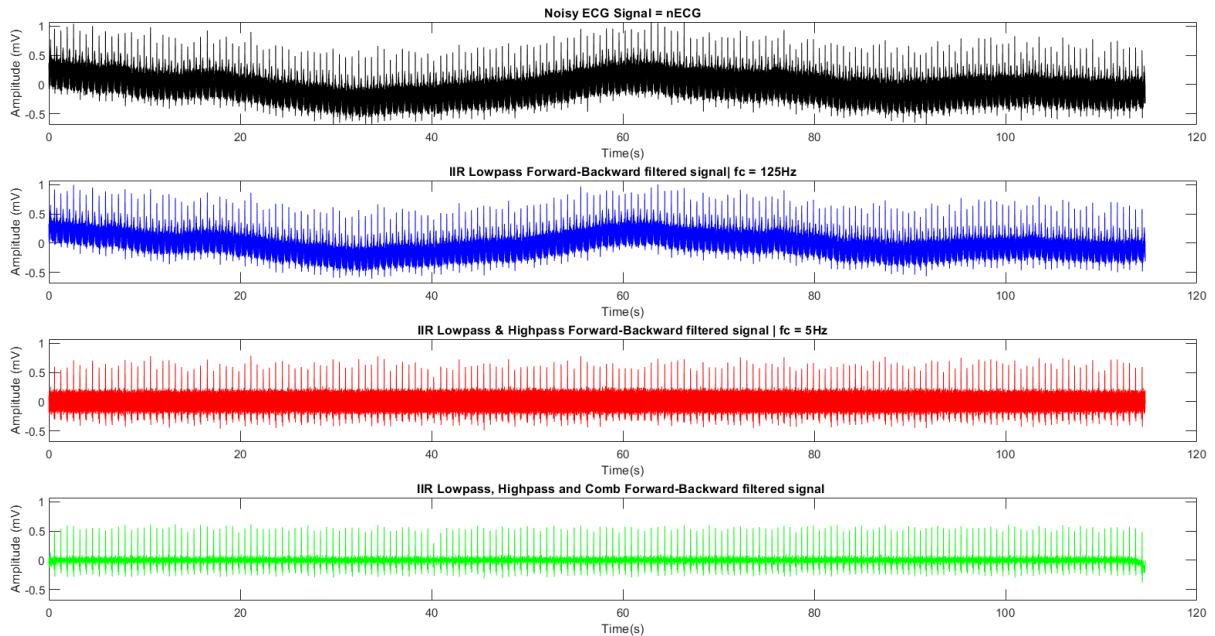


Figure 64: Forward-Backward Filtered Signal

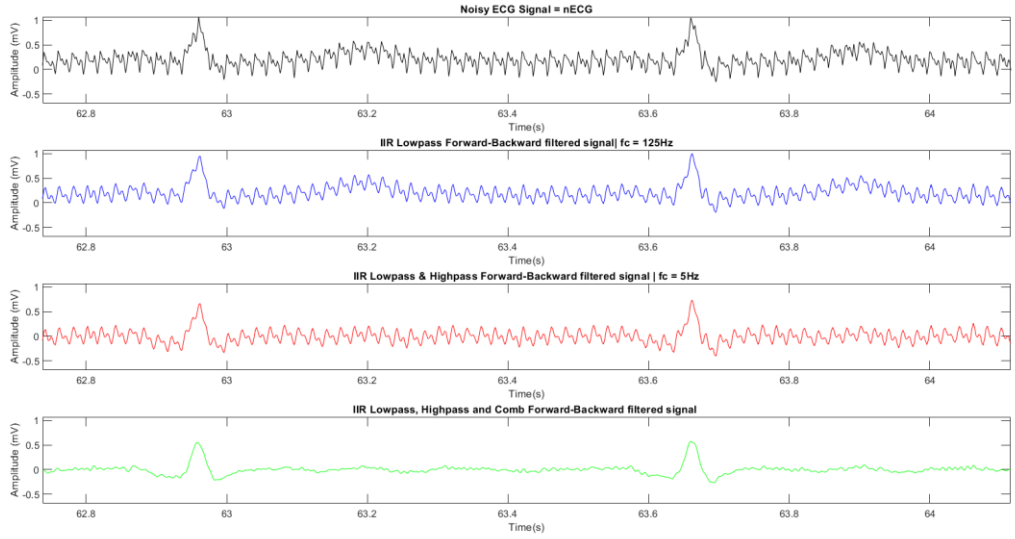


Figure 65: Forward-Backward Filtered Signal (Zoomed)

By looking into the Figure 65, we can see that the signals have aligned each other in the time axis which implies that the Forward-Backward Filtering is able to remove the group delay effect appeared in Forward Filtering. See Figure 66.

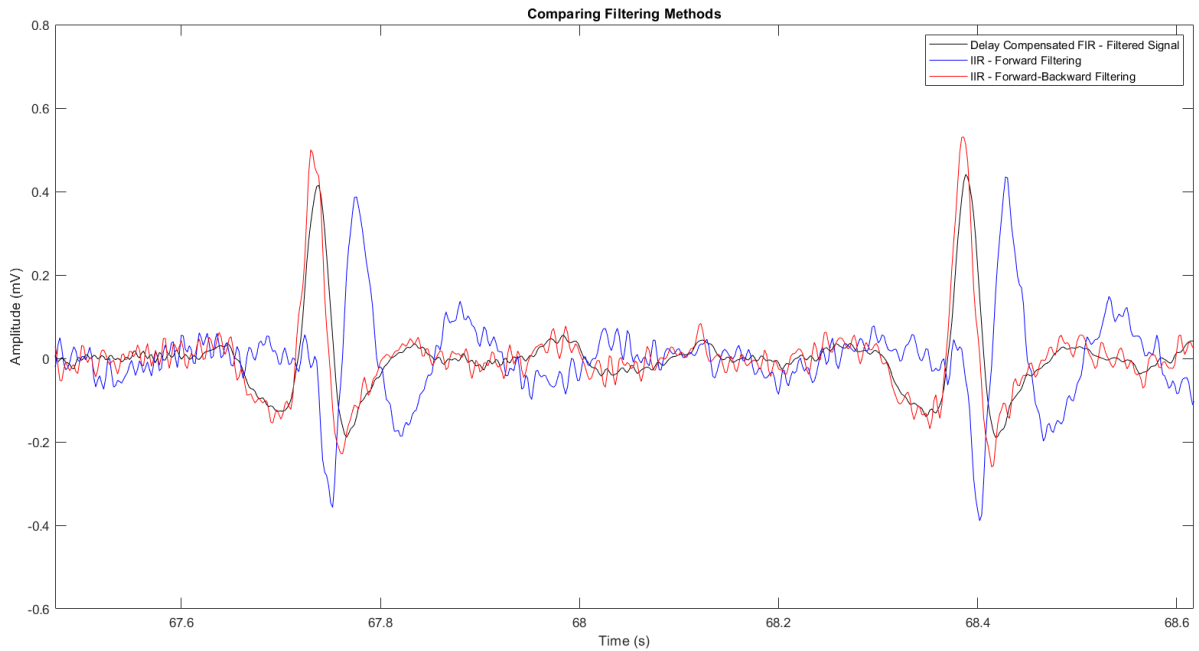


Figure 66: Filter Comparison

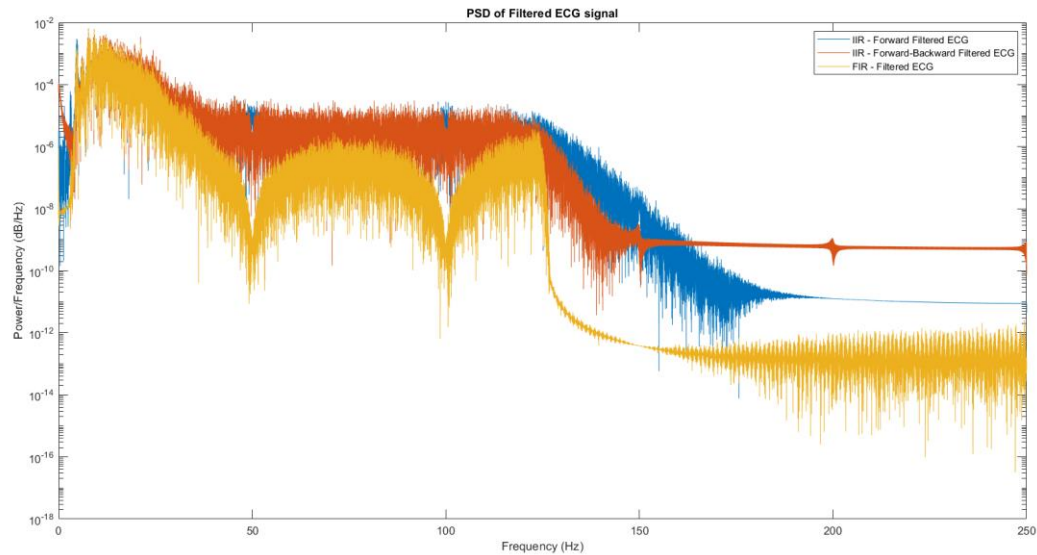


Figure 67: PSD Comparison

Referring to Figure 67, we can see that IIR filters attenuates low signal power in the pass band. Also, the FIR notch filter removed higher number of frequency components compared to IIR filtered signal due to the wider notch.